Title

SYNTHESIS OF LOW TEMPERATURE STABLE A15 COMPOUNDS IN THE NIOBIUM SYSTEM

Author

Hazra, Subhas.

Publication Date

1971-12-01

Thesis/dissertation

LBL-433

SYNTHESIS OF LOW TEMPERATURE STABLE A15 COMPOUNDS IN THE NIOBIUM SYSTEM

Subhas Hazra
(M.S. Thesis)

December 1971

AEC Contract No. W-7405-eng-48

LBL-433

DISCLAIMER

Table of Contents

SYNTHESIS OF LOW TEMPERATURE STABLE A15 COMPOUNDS IN THE NIOBIUM SYSTEM

Subhas Hazra

Inorganic Materials Research Division, Lawrence Berkeley Laboratory and Department of Materials Science and Engineering, College of Engineering University of California, Berkeley, California

ABSTRACT

The A15 phases of the Nb-Ge, Nb-Ga and Nb-Si systems were investigated. By low temperature vapor deposition the A15 phase boundary of NbGe and NbGa was extended towards the stoichiometric composition; the T_c onset was 15.2°K and 16.5°K respectively. The lattice parameter showed a decrease as the 3:1 composition was approached.

The A15 structure was observed in the Nb-Si system for the first time. Nb_3Si transforms to tetragonal above 680°C. No high T_c has been observed so far but some annealing methods which might lead to higher T_c are proposed.

I. INTRODUCTION

The fact that niobium has the highest superconducting temperature among all the elements in their normal state and its presence among those compounds with highest T_c, inspired us to investigate the β-W phases in the different systems of the element. In our search for high superconducting binary alloys we have investigated the Nb-Ge, Nb-Ga and Nb-Si systems.

Müller[1] et al. had prepared Nb_3Ge with a highest T_c of 5.5°K, at 18 at.% Ge composition, claimed as the maximum solubility of Ge in the β-W Nb_3Ge phase. Later (in 1965) Matthias[2] and his co-workers were able to extend the A15 phase to higher Ge concentrations by splat cooling techniques and thereby obtained T_c as high as 17°K. By vapour deposition on low temperature substrates it has been possible to extend the A15 Nb_3Ge phase towards the stoichiometric 3:1 composition and thereby obtain T_c onset at 15.20°K. With the hope of extending the Ga content in the β-W Nb_3Ga phase by the same technique, an investigation was made of the Nb-Ga system. During the process of our experiments G. Webb[3] et al. claimed to have obtained a stoichiometric Nb_3Ga with superconductivity above 20°K. They had obtained the stoichiometric material by quenching from above a solidus followed by a low temperature anneal. We have also been able to extend the A15 phase towards the stoichiometric material and have obtained a T_c onset at 16.5°K.

J. J. Hopfield's[4] suggestion that a β-W phase with a small atomic volume (leading to a small Nb-Nb distance) could give high superconducting temperatures, inspired us to investigate the Nb-Si system. Since

the atomic radius of Si is much smaller than Nb, it seemed reasonable to assume that if a β-W Nb_3Si phase existed, then it would have a small atomic volume, leading to a high T_c. The existence of β-W Nb_3Si was judged not possible according to M. V. Nevitt[5] because of a unfavorably large R_A/R_B. D. K. Deardorff and co-workers[6] had attempted to form Nb_3Si in the β-W crystal structure, but instead discovered tetragonal Nb_3Si. The tetragonal Nb_3Si exists at stoichiometric 3:1 composition below 1945°C. A claim by Galasso and Pyle[7] of a Nb_3Si with f.c.c. structure (with a low superconducting transition temperature of 1.5°K) was discarded by Deardorff et al. because of their 99% pure materials.

The possibility of existence and stabilization of A-15 phases by vapor deposition at low temperatures suggested by L. D. Hartsough and R. H. Hammond[8] encouraged the search for β-W Nb_3Si under these conditions. The results were the first to establish the existence of β-W Nb_3Si stable below 680°C with a lattice parameter $a_o = 5.170 \pm 0.001$Å. Attempts to measure the solid-solubility of Si in Nb had been fruitless because of highly disordered amorphous like nature of the films. The T_c measured was not up to expectations for the same reason. However methods of annealing to obtain better ordering or the β-W Nb_3Si phase, which might lead to a high superconducting temperature, have been proposed.

II. EXPERIMENTAL

A. Apparatus

1. Vacuum Chamber

The vacuum chamber was a three foot diameter by a 3 foot long water cooled stainless steel horizontal cylinder. A liquid nitrogen baffled 12 in. oil diffusion pump backed by a mechanical pump was used for pumping down. During the pump down the chamber could be outgased by circulating water at 100°C through its cooling coils. The ultimate pressure achieved by the diffusion pump was in the lower range of 10^{-7} torr as read by a Veeco RGLL-6 ion gauge.

2. Evaporation Sources

Materials to be evaporated were held in separate water cooled copper crucibles, and electron beam heated by Temescal 180° magnetic deflection electron beam guns operated at 10 kV. With the localized surface heating provided by electron bombardment the element served as its own crucible and thus the contamination from the copper crucible was minimized. Table I shows the purity of the materials used.

The flux of each element was monitored by a Allen-Jones Mark I chopped-beam ionization type rate monitor and controlled by a feedback loop to the electron beam source. With this technique, the ratio of the elements arriving at the substrates was kept constant to within a few percent during the time required to deposit the samples. To convert the reading of the rate monitor from ERM (arbitary units) to Å/sec, the monitor had to be calibrated for each geometry and element used.

Table I. Purity and Source of Materials

Material	Source	Nominal Purity	
Ga	United Mineral & Chemical Corp.	99.99	lumps
Ge	"	higher than 4N	ingot
Si	"	99.99	$\frac{3}{4}$ in. dia. pieces
Nb	-	99.82%	ingot

Thus, the approximate composition at a particular place on the substrate was ensured.

3. Substrate Holder

A tantalum block 6 in. long and 1 $\frac{1}{2}$ in. wide with grooves to hold 6 substrates each 1 in. × 1 in. was mounted above the evaporation guns, behind a shutter which could be controlled from outside the chamber. The block was provided with (a) a Chrome Alumel thermocouple soldered just behind the base plate supporting the substrates and (b) a tungsten heating coil 6 in. long. Thus the substrate deposition temperature could be varied and measured.

4. Substrates

The substrates were 1 in. × 1 in. × $\frac{1}{16}$ in. polycrystalline Alumina Superstrates supplied by Materials Research Corporation. The substrates were cleaned by first placing them in an ultrasonic cleaner containing Labtone soap solution for fifteen minutes then in boiling hot water for another fifteen minutes. They were then rinsed in boiling distilled water, followed by Ethanol and finally dried in air dryer.

5. Critical Temperature Measuring Probe

A schematic of the circuits used to measure the germanium thermometer and sample resistances is shown in Fig. 1. Copper (No. 36 wire) current and voltage leads were attached to copper Berylium strips which made four point pressure contact with the substrates. Two substrates at a time were held in the grooves made on a copper block

which was fixed to the end of a long metal tube. Two germanium thermometers were fixed behind the two substrate positions. The whole set up was then gradually immersed in a liquid Helium dewar. The sample measuring current was 0.1 milliamperes dc. The current could be manually reversed to eliminate the effects of zero drift. The sample voltage was measured with an Astro data (Model 121RZ) nanovoltmeter whose output was displayed on the y-axis of an electro Instruments x-y recorder (Model 520). The thermometer measuring current was 10 microamperes d.c. The thermometer voltage was displayed on the x-axis of the recorder. This was calibrated in terms of resistance by displaying the voltage across the standard resistors in series with the thermometer and the constant dc measuring current supply.

6. Annealing Furnace

The annealing furnace was a two feet diameter 3 feet high stainless steel vertical bell-jar resting on a 2 feet diameter base plate. The bell-jar could be mechanically lifted from the base plate. The samples were placed on a tantalum box 6 in. × 1 in. above a 6 in. long tungsten heating coil and then covered by another tantalum case which served as a heat shield. The tantalum box was placed on a platform two feet above the base plate supported by three stainless steel rods. The cylinder was provided with a double walled liquid nitrogen shroud which served as the inner wall of the furnace. Besides the diffusion pump the furnace was equipped with the Torrgett titanium high-vacuum pump from Veeco Instruments Incorporation. During annealing the pressure was in

the range of 10^{-9} Torr as read by a Veeco RG-31A type ionization gauge. For optimum performance of the Torrgett pump it was recommended to have the wall temperature below room temperature.

B. Experimental Procedure

1. Nb Calibration

This was simply done by evaporating niobium from the copper crucible with the 180° electron beam gun with an arbitarily chosen rate monitor setting. The evaporation was carried out for 15 seconds. Both the crucible and the gun were placed at one end of the substrate holder during the evaporation. The substrates which were held at 150°C during evaporation were then allowed to cool. All the six substrates were numbered serially from one to six and then coated with a thin aluminum film. The height of the step caused in the shiny aluminum film by the niobium deposit was then measured with a multiple beam interferometer (Varian Å scope). The variation in thickness with the distance from the Nb source was determined. It was then a simple matter to convert the thickness to Å/sec. Thus the variation of Å/sec deposit of niobium on the substrates relative to its distance from the niobium source for a definite rate monitor setting was determined.

2. Ga, Ge, and Si Calibration

The metal for which the rate monitor had to be calibrated was taken in a glassy carbon crucible and evaporated. The same procedure was followed as in the case of niobium, except with a basic difference. The crucible and the electron beam gun were placed towards the other end of the substrate holder. The significance of this basic change is

explained later on. Once the two rate monitors had been calibrated the evaporation rates could then be so adjusted that any particular composition could be deposited on any particular position on the substrate as desired. The accuracy of this adjustment was surprisingly high and was in good agreement with the microprobe data.

3. A15-Phase Deposition

Niobium and the other alloying element were placed in two different crucibles with two electron beam guns and placed in the same positions as they were during the time of calibration. Six clean 1 in. × 1 in. alumina substrates were placed in the substrate holder and the substrate shutter was closed. The vacuum chamber was then closed and evacuated. Hot water at 100°C was circulated through the chamber's cooling coils. After 10 hrs the chamber pressure reached 1×10^{-6} Torr. The hot water was then turned off and cold water was circulated. After 30 to 45 minutes when the chamber walls were cold the substrate heater was turned on and held at the desired temperature for 15 minutes. By this time the pressure had reached 2.0×10^{-7} Torr. The high voltage was then turned on and the metals were melted by their respective electron beam guns. The filament current of the electron beam guns were further increased till both the rate monitors reached the desired rates and then the automatic rate control was turned on. The substrate shutter was opened for three minutes and then closed. The rate monitor automatic control was immediately turned off and the electron gun filament current was decreased. The substrate heating power was immediately turned off to minimize possible contamination of the deposits.

The high voltage was then turned off and hot water was circulated through the cooling coils of the chamber. After the chamber had warmed to the room temperature the substrates were taken out and the critical temperatures were measured at different compositions.

The use of an extended substrate and the geometric displacement of the two metal sources towards the two ends of the extended substrate made it possible to make, in a single experiment, a considerable portion of the binary phase diagram.

4. T_c Measurements

The composition of the alloy changes along the length of the substrates. In order to measure T_c on an approximately constant composition, the substrates were cut with a diamond scriber into narrow strips of $\frac{1}{4}$ in. width. The difference of composition across the width of the strip was approximately 1 at.% as obtained from the microprobe data. The samples were loaded on the copper block of the T_c probe and gradually immersed in the liquid helium dewar. The start of the superconductivity or the onset temperature was accompanied by a voltage drop across the sample. This voltage drop was displayed on the y-axis of the x-y recorder. When the sample was completely superconducting the voltage dropped to zero. Though the normal convention is to use the temperature at the mid-point of the signal as the superconducting temperature, the results given herein are in terms of the onset temperature and the completely superconducting temperature, so that the transition width can also be seen simultaneously. As a preliminary check of the equipment, a Nb film was deposited on an alumina substrate

held at 400°C, under a pressure of 4.0×10^{-7} Torr with 0.4×10^{-7} ERM (arbitary unit) rate of evaporation for a period of 2 minutes. The T_c of the film was then measured to be 9.6°K. The T_c of bulk Nb is 9.2°K, but some investigators have reported 9.4°K for disordered Nb. The Ge thermometer calibration was then checked in liquid hydrogen and liquid He. The temperatures measured were in good agreement with the calibrated values.

5. X-ray Measurements

X-ray diffraction patterns of films three microns in thickness were taken on a Picker x-ray diffractometer. Nickel-filtered Cu-K radiation combined with a scintillation counter and pulse height discrimination was used for lattice parameter measurements. The substrate lines, which were obtained together with the characteristic lines of the film deposit were accounted for by comparison with an x-ray diffraction pattern on the superstrate alone using the same Ni filtered Cu K radiation and Time Constant = 1. A slit width of 1° was used for low angle lines which was replaced by a 2° slit for higher 2θ values, in order to get high intensities at these angles.

The A15 phase boundary at the Nb deficient side was determined by observing the strongest line of the Nb_5Ga_3 and Nb_5Ge_3 solid solution phases in their respective alloy systems. The lattice parameter of the A15 phase was measured on the composition where the above mentioned lines were just begining to appear. The lattice parameter was computed from 10 values of 2θ using $\lambda(CuK\text{-}\alpha) = 1.54178\text{Å}$ and a least square

extrapolation was made on a vs $1/\sin 2\theta$. Since the high angle lines were very broad and occurred adjacent to the substrate lines, futile attempts were made to resolve the $k\alpha_1$ and $k\alpha_2$ peaks by the error function. Furthermore a_o determined by a plot of a vs Taylor Sinclair function for high angles showed good agreement with those obtained by the above mentioned method in some cases.

6. Microprobe Analysis

Microprobe analysis was performed on the films in an effort to determine the compositions of the phases present. A Materials Analysis Company three-counter microprobe was used. The films were thicker than the infinite thickness required for these elements, so a correction for film thickness was not deemed necessary. The (I_o) of Nb, Ge, Ga and Si were determined by measuring the intensities of $Nb(L_\alpha)$ $Ge(K_\alpha)$ $Ga(K_\alpha)$ $Si(K_\alpha)$ from pure Nb, Ge, GaSb with 50 at.% Ga, and pure Si respectively. For quantitative analysis, ratios of net x-ray intensities from the samples to those obtained from pure elements (I/I_o) were calculated. For Ga, the 50 at.% Ga in the GaSb alloy was converted to wt.% Ga and then (I/I_o) was determined. Absorption corrections were calculated by the method of Philbert[9] as modified by Duncumb and Shields.[10] Atomic number corrections were made only for the NbSi alloys as suggested by Bishop.[11] Heinrich's[12] absorption coefficients were used for all the elements.

7. Annealing

The operation of the annealing furnace was similar to the operation of the evaporation chamber. The main difference was that liquid nitrogen was circulated in the shroud for cooling, and heating

filaments made of tungsten were used for baking the furnace. After the samples were placed in the tantalum box the furnace was baked and pumped for 12 hrs, with air blowing through the shroud. After 12 hrs when the pressure was 1×10^{-7} Torr, the shroud was filled with liquid nitrogen and the torrgett pump was started. When the pressure reached 1×10^{-8} Torr the sample heater was turned on (Thermac Controller Model MPR). After the desired time of annealing the sample heater was turned off. When the temperature reached 100°C the Torrgett pump was shut off. The liquid nitrogen circulation was stopped and air was blown through the shroud. The bake out was then turned on to bring the walls of the furnace to the room temperature. Just before opening the furnace the bake out was stopped and helium gas was admitted from the bottom of the furnace.

With every set of samples a niobium film was annealed. A change in T_c of the annealed niobium is an indication of oxidation during the annealing. A T_c value of 8.6°K for the Nb annealed film was usually measured. This could be attributed to the oxidation of Nb, even at 10^{-9} Torr pressure. However it is believed that Nb is much more susceptible to oxidation than the A15 compounds.

C. Results and Discussion

1. Nb-Ge System

a) The niobium and germanium were deposited on six alumina substrates under a pressure of 2×10^{-7} Torr. Deposition rates were 1 micron per minute. Three such evaporation runs were made with substrate temperatures at 600°C, 420°C and 300°C. The evaporation

was carried out for a period of approximately three minutes during each run, thus depositing films of about three microns in thickness. Table II shows the conditions of deposition of the three samples. X-ray diffraction data enabled us to determine the following phases in decreasing order of their Nb content: A2 (b.c.c.) solid solution the A15 phase and the Mn_5Si_3 type hexagonal Nb_5Ge_3. These different regions were visually apparent because of their differences in color. The A2 phase was yellowish, the A15 was light gray and the Nb_5Ge_3 was dark gray. The mixed phases between the solid solution regions had a mixture of the colors of the solid solutions at its two extremeties. X-ray diffraction pattern were taken on different positions of the substrates and the A15 phase boundary on the Ge rich side was determined for all the three sets of runs. The 2θ values of the A15 lines measured on the phase boundary were observed to shift to higher angles with decreasing substrate temperatures. Since the Ge atoms are smaller than the niobium atoms (1.444Å and 1.456Å) respectively, an increase in Ge at.% results in a decrease of the lattice parameter which is displayed by a 2θ shift to higher angles. These observations were consistent with the microprobe data which showed an increase in the Ge at.% at the A15 phase boundaries with decreasing deposition temperatures. Figure 2(a) shows the Ge at.% of the Ge rich side A15 phase boundary vs. deposition temperatures. Figure 2(b) shows the lattice parameter measured on the A15 phase boundary vs at.% germanium. The ordering of the A15 phase deteriorated with decreasing deposition temperatures. The A15 phase of the 300°C deposition temperature film

Table II. Evaporation Conditions for Nb-Ge System.

Deposition Temperature	Chamber Pressure [Torr]	Rate of Evaporation ERM (arbitary unit)		Duration of run [min]
		Nb	Ge	
300°C	3.2×10^{-7}	0.4×10^{-7}	0.175×10^{-7}	$3\frac{1}{2}$
420°C	4.3×10^{-7}	0.4×10^{-7}	0.125×10^{-7}	3
600°C	2.0×10^{-7}	0.4×10^{-7}	0.15×10^{-7}	$3\frac{1}{2}$

was so disordered that the lattice parameter could not be measured although the existence of the phase at this composition could be determined by the disappearance of the strongest Nb_5Ge_3 line. The amount of ordering of the A15 phase at the phase boundary with deposition temperatures at 300°C and 420°C can be seen in Figs. 3 and 4 respectively.

T_c was measured at different compositions from 16-35 at.% germanium, for all the three sets of runs. A peak in the T_c onset value was determined on the A15 phase boundary compositions which varied with the deposition temperature. The T_c onset peak values for different runs are plotted vs composition in Fig. 2(c). Films with different compositions were then taken from all the three runs and annealed at 700°C for 24 hrs. T_c vs composition was then plotted for the three sets of runs. The T_c onset peaks were observed to be higher than those on as deposited films, but the compositions at the T_c onset peaks were same as in the 'as deposited' films. T_c onset peak values for the three runs after 24 hrs anneal at 700°C are plotted against Ge at.% compositions in Fig. 2(d). The data plotted in the figures are complied in Table III. Figure 2(e) shows the at.% Ge vs lattice parameter. The line AB shows the values obtained by Müller[1] et al. C'D' and A'B' are drawn parallel to AB. The data points near the line A'B' and C'D' were taken from the 600°C and 420°C deposition temperature runs respectively.

b) Discussion. Müller[1] et al. had investigated the Nb-Ge system and had observed the same colors of the A2(b.c.c.) A15 and Nb_5Ge_3 solid solution phases, as we had in our films. The measured 2θ values

and the line intensities of the A15 phase agreed well with those observed by M. V. Nevitt.[13] Although Müller suggests the A15 phase at 1600°C to lie between 18-13 at.% Ge with T_c between 4.4°K and 5.5°K respectively, Matthias et al.[2] had by rapid quenching made a closer approach to the stoichiometric 3:1 composition and thereby increased the T_c onset to 17°K, as indicated by slight change in resistivity. Extension of solubility in metastable phases by vapor quenching was also observed by P. Duwez et al.[14] This method was first used by Buckel[15] and Hilsh[16] and others[17] to obtain many interesting metastable structures in thin films. Matthias et al. had samples prepared by conventional arc melting and annealing techniques with nominal compositions including 25 to 29 at.% germanium. All had rather sharp transitions at about 6°K. When these alloys were rapidly quenched (cooling rates in excess of 2×10^6 deg/sec) by argon splattering against a massive copper shield on the far side of the arc furnace, the start of the high temperature transition was pronounced and increased with increasing quenching speeds to 17°K. The maximum transition temperatures were reached near the compositions from 25 to 29 at.% Ge. Higher and lower germanium concentrations had lowered the transition temperature. We have observed a peak in the T_c onset only at one particular composition i.e., at the A15 phase boundary in all the three sets of runs at their respective deposition temperatures. See Table III, Col. 2 and 4. Matthias et al., suggested that, although this quenching method increases the solubility of one element in another, there is also a possibility of producing disorder. This explains the high disorder of the 300°C deposition temperature

Table III. T_c before and after anneal, lattice parameter and Ge concentrations measured at the Ge rich side A15 phase boundary.

Deposition Temperature	[At.% Ge] at A15 phase boundary	Lattice Parameter at A15 phase [Å]	'As deposited' Transition Temperature		Anneal 700°C 24 hrs. Transition Temperature	
			Start	End	Start	End
600	24	5.191 ± 0.001	7.3	5.1	7.3	5.1
420	24.5	5.170 ± 0.001	13.57	9.20	14.9	11.25
300	25		4.5	4.2	15.2	13.25

sample (Fig. 3), and consequently the low T_c onset. In the other 2 samples where the ordering is the same, the A15 phase boundary composition is the criteria for T_c and as can be seen from Fig. 2(c), it increases with low deposition temperatures and high Ge concentrations at the phase boundary. Matthias et al. predicted that a heat treatment at elevated temperatures would not be expected to improve the ordering since the metastable stiochiometric alloy would decompose to a composition having a lower superconducting transition temperature.

This however depends upon the amount of disordering and the temperature of anneal. The 300°C deposition temperature sample had improved ordering after the anneal. This was seen from x-ray diffraction lines. Since it had well ordered A15 and closer approach to 25 at.% Ge, a higher T_c compared to 'as deposited' was observed. The 420°C sample also showed some ordering in the x-ray analyses whereas the 600°C sample was so well ordered in the as deposited state that a further improvement of ordering was not perceptible after the annealing. The unchanged T_c onset before and after anneal can be understood from the Matthias prediction. Since all the samples had the same degree of ordering of the A15 phase after the annealing the Ge concentration was the main criteria for a high T_c (this can be seen from Fig. 2(d)). The T_c increases with closer approach to 3:1 composition.

A x-ray diffraction pattern taken on the 300°C deposited sample after 24 hrs anneal at 700°C is shown on Fig. 5. The lattice parameter measured was 5.163Å ± 0.001Å. Slight indication of Nb_5Ge_3 was also observed, so a higher temperature anneal was not done on these-samples.

The highest T_c onset obtained at 15.2°K compared to Matthias's 17°K was attributed to the problem encountered with the Nb evaporation rate, discussed in the General Discussion Section.

2. Nb-Ga System

a) The niobium and the gallium were evaporated from two different crucibles and the films were deposited on alumina superstrates. The rate of evaporation was 1 micron per minute. Four such runs were made with different deposition temperatures. Table IV shows the conditions of deposition of the films. The film thicknesses were approximately 4 microns. The x-ray analysis showed the line systems of α-Nb, β-W phase Nb_3Ga, and the tetragonal phase Nb_5Ga_3[18] on the films with increasing Ga content respectively. The A15 phase boundary on the Ge rich side was determined by the 'disappearing phase' method, which was done by noting the disappearance of the strongest Nb_5Ga_3 line. Microprobe analysis was performed to determine the composition of the alloy at the A15 phase boundaries at different deposition temperatures. An extension of the A15 phase boundary towards higher Ga content with decreasing deposition temperatures was observed. This observation was consistent with the lattice parameter measurements, which gradually decreases with increasing Ga content. Figure 6(a) shows the deposition temperature vs. the at.% Ga and lattice parameters measured at the A15 phase boundary (Ga rich side). The film deposited at 700°C just after evaporation was held at 700°C for 18 hrs. in the evaporation chamber. The as-deposited data shown in Fig. 6(a) for this run is, strictly speaking, after the 18 hrs. anneal at 700°C.

Table IV. Evaporation Conditions for Nb-Ga System.

Deposition Temperature	Chamber Pressure [Torr]	Rate of Evaporation ERM (arbitary unit)		Duration of run [min]	Comments
		Nb	Ga		
167°C	3.0×10^{-7}	0.42×10^{-7}	0.175×10^{-7}	4	-
459°C	2.5×10^{-7}	0.33×10^{-7}	0.175×10^{-7}	5	-
700°C	3.0×10^{-7}	0.35×10^{-7}	0.175×10^{-7}	5	(Annealed at 700°C-18 hrs)
1064°C	3.0×10^{-7}	0.4×10^{-7}	0.17×10^{-7}	$4\frac{1}{2}$	-

Critical temperatures were measured on all the runs at different compositions. The highest T_c onset peak was determined at the Ga rich side of the A15 phase boundary for the respective deposition temperatures. The 167°C deposition temperature run showed a T_c onset at 8.8°K over a broad range of composition between 20-25 [at.%] Ga. Figure 6(b) shows the T_c onset peak values vs. lattice parameters. The films were then annealed at 220°C for 2 hours. The T_c onset peaks were found at the A15 phase boundary compositions for all the runs. The 167°C deposition run had an improved T_c onset from 8.8°K on 'as deposited' to 15.2°K after annealing. The T_c of the 459°C run rose from 10.90°K to 12.12°K. The other 2 samples did not show any improvement after this anneal.

Samples were then taken from the 167°C run at different compositions and annealed for 24 hrs at 620°C. The highest T_c onset measured after this anneal was 16.5°K at the 25 [at.%] Ga composition, compared to 8.8°K measured on the 'as deposited' film. Compositions with higher Ga content showed lower but fairly good T_c onset temperatures. T_c measured on the 30 at.% Ga had a T_c onset at 13.7°K compared to 4°K measured on the 'as deposited' film. X-ray diffraction patterns taken at this composition before (Fig. 7) and after anneal (Fig. 8) showed improved ordering of A15 together with the Nb_5Ga_3 lines. As deposited samples were taken from runs 1064°C, 700°C and 167°C and annealed at 700°C for 24 hrs. The 450°C run samples were exhausted and therefore could not be taken for this annealing. The highest T_c onset measured in every set of runs was at the composition with lowest lattice

Table V. T_c before and after anneal, and lattice parameter measured at the Ga rich side A15 phase boundary.

Deposition Temperature	Lattice Parameter at A15 ph Boundary on the Ga Rich side 'As Deposited'	As Deposited Transition Temperature		After 24 hrs Anneal at 700°C Transition Temperatures	
		Start	End	Start	End
1064°C	5.182 ± 0.003	15.20	13.17	15.20	13.70
700°C	5.188 ± 0.001	11.50	9.41	12.10	11.20
459°C	5.181 ± 0.001	10.90	8.80		
167°C	5.175 ± 0.001	8.8	7.0	16.50	12.80

parameters in the as deposited state. The 167°C run had the highest T_c onset at 16.5°K. There was no improvement in T_c compared to that after 620°C anneal. X-ray analysis performed in these films showed improved ordering for the 167°C and 700°C run compared to the as deposited samples. The 1064°C run was fairly well ordered as deposited, so a marked change after this 700°C annealing could not be observed. The lattice parameter of the annealed 167°C run at the 25 at.% Ga composition was 5.172 ± 0.002Å compared to 5.175 ± 0.001Å on the as deposited film.

b) Discussion. G. W. Webb[3] et al. had investigated the Nb-Ga system in the R. C. A. Laboratories and had been successful in obtaining T_c above 20°K in stoichiometric Nb_3Ga. They had a sample with nominal 32 at.% Ga and quenched it into liquid Ga from above its liquidus temperature. The particle size of the quenched material was below the resolution of the optical microscope. Annealing at 700°C for 24 hours caused T_c to rise to 20.3°K and the lattice constant of the β-W phase to decrease and to sharpen. The mean value of the β-W lattice constant was 5.165Å. To determine the composition of the β-W phase, they prepared two samples of different compositions by annealing near their solidus points. After making a materials balance, the compositions and the lattice parameters were determined to be 19.3 ± 0.5 at.% Ga, a_o = 5.178Å and 23.0 ± 0.5 at.% Ga, a_o = 5.170Å. Assuming a linear dependence of a_o on composition, for a_o = 5.165Å they had determined the extrapolation composition to be at 25.3 ± 1.0 at.% Ga. From (Fig. 6(a)) a_o at 20 ± 1 at.% Ga and 25 ± 1 at.% Ga are 5.188Å and

5.175Å respectively. The difference in the absolute values can be partly attributed to the function used in the computer to determine the a_o values. The R. C. A. paper does not give any details of their method of lattice parameter measurements. Our computer program for the a_o measurement was made on the basis of a vs $1/\sin 2\theta$. For a further check we have plotted a vs the Taylor Sinclair function for higher angle lines. In some cases the extrapolated a_o was in good agreement with the computer calculations. But in other cases it showed random deviations. Possibility of other errors involved are discussed in the General Discussion Section.

Nevertheless a highest T_c onset of 16.5°K was measured at the lowest lattice parameter, and with the increase in lattice parameter the T_c onset started decreasing Fig. 6(c).

On the as deposited films (Fig. 6(b)) the substrate temperature controlled the T_c onset. The T_c onset increased with increasing substrate temperatures. At lower substrate temperatures the vapor atoms condensed spontaneously at or near the point of impingement on the substrate. At higher substrate temperatures the atoms could arrange themselves to better ordered crystallites.

Though it was possible to extend the A15 phase towards stoichiometric 3:1 composition on the low substrate temperature depositions, disordering also increased simultaneously. After the 24 hrs anneal at 700°C, when the low temperature films had the same ordering as the high temperature films, the T_c onset was controlled by the Ga content of the A15 phase.

The films with 700°C deposition temperature were made by evaporating Nb and Ga for 5 minutes on alumina substrates. The high voltage of the electron beam guns were then turned off, but the substrate temperature was held at 700°C for 18 hrs. The sudden drop of Ga solubility in the A15 phase after this anneal is unexplained (See Fig. 6(a)). The 167°C run, which was annealed at 700°C for 24 hrs (though not immediately after the deposition of the film) showed no change in lattice parameter, before and after the anneal. However the increase in T_c onset with the decrease in lattice parameter was overall observed.

3. Nb-Si System

The niobium and silicon were deposited at various substrate temperatures. The low temperature deposits had highly disordered structures which gradually changes over to A15 structures with increasing deposition temperatures. The disordered structures had a single very broad peak in the x-ray diffraction pattern, with no indication of any ordered structure. Though it is hard to draw a line between amorphous and highly disordered phases, for the sake of convenience this highly disordered phase will henceforth be denoted as the amorphous phase in our further discussions. Table VI shows the conditions of deposition of our samples. A Debye-Scherrer powder pattern, using material scraped off from the 21 (at.%) Si composition of the glass substrate deposition, was taken. All the lines expected of the A15 phases were observed. Nickel-filtered λ(Cu-Kα) = 1.54178Å radiation was used for lattice parameter measurements. The lattice parameters were plotted vs. $1/\sin 2\theta$ and the $a_o = 5.170 \pm 0.001$Å was determined by the computed

Table VI. Evaporation conditions for Nb-Si system.

Deposition Temperature	Chamber Pressure [Torr]	Rate of Evaporation [ERM] Nb	Rate of Evaporation [ERM] Si	Duration of Run [mins]	Substrate Material
100°C	3.0×10^{-7}	2.0×10^{-8}	0.35×10^{-8}	7	Alumina Superstrate
140°C	3.0×10^{-7}	2.0×10^{-8}	0.29×10^{-8}	8	Alumina Superstrate
220°C	2.0×10^{-7}	2.0×10^{-8}	0.24×10^{-8}	10	"
450°C	2.0×10^{-7}	2.0×10^{-8}	0.175×10^{-8}	16	"
530°C	3.0×10^{-7}	2.0×10^{-8}	0.22×10^{-8}	10	Glass
1000°C	2.0×10^{-7}	2.0×10^{-8}	0.22×10^{-8}	16	Alumina Superstrate

Table VII. Observed and Calculated Intensities of β-W Nb_3Si phase measured at 21 (at.%) Si composition.

hkℓ	2θ	I_{obs}	I_{calc}
110	24.38	20	37.69
200	34.71	45	37.70
210	38.86	290	286.67
211	42.76	100	100.00
220	50.02	11	10.69
310	56.02	16	16.43
222	62.17	44	65.28
320	64.99	77	97.30
321	67.67	77	75.37
400	73.20	50	52.03
420	83.76	33	25.78
421	86.18	94	117.76
332	88.62	28	24.03
520	107.06	50	55.31
521	109.61	44	47.00
440	115.04	78	80.86
600	127.00	11	7.48
610	130.31	15	77.8
611	133.50	22	34.59

least squares extrapolation. The highest 2θ value used was 133.50°. Both the positions and the line intensities of the observed peaks were taken from a microphotometer trace of the powder pattern. Table VII shows the line positions and intensities measured from the film. The observed and the calculated intensities are in fairly good agreement. Figure 9 shows the amount of random orientation of the sample used for intensity measurements.

The relative integrated intensity was calculated by a computer program. Sin θ/λ was calculated for all the observed lines and then the atomic scattering factor was calculated. Given the β-W structure the structure factor was determined for each (h,k,ℓ). Then from Lorentz Polarization factor and multiplicity factor of each (h,k,ℓ), the relative integrated intensities were calculated. Although (210) has the maximum relative integrated intensity, since Nb A2(bcc) has a high reflection at this 2θ value, the (211) was calibrated as 100.

The I_{obs} was calculated by measuring the area under the peaks above the background, in the microphotometer trace of the Debye Scherrer film and compared with the area under the (211) peak.

The structure of the film deposits determined by x-ray diffraction were seen to change pattern with deposition temperatures as follows:

Dep. Temp.	Structure	Compositions [at.%] Si
100°C	Amorphous	25
140°C	Amorphous	25
220°C	Amorphous	25
450°C	A15 (broad lines)	25
530°C	A15 (narrower lines)	25
1000°C	Tetragonal	25

The Figs. 10(a)-(e) show the change in structures with change in composition of the sample deposited at 100°C. A15 lines observed in the 2 phase region with 11 at.% Si gradually became disordered and finally turned amorphous at compositions higher than 17 at.% Si. With higher deposition temperatures the start of the amorphous phase shifted towards higher Si contents. Figure 11 shows the sample deposited at 530°C had the A15 structures at 25 at.% Si.

The highest T_c so far measured with the as deposited films was 9.3°K for the run with 530°C deposition temperature and the 21 at.% Si specimen. Both the A2(b.c.c.) and A15 phases were present in this specimen. With increasing Si, the A15 became progressively disordered; the T_c onset began to drop and finally, with the appearance of the amorphous phase, the T_c onset was not detectable at 5.5°K (the lowest test temperature). The T_c onset at 25 at.% Si in the 530°C deposition temperature run was 9.1°K whereas the same composition on the 140°C deposition temperature film had no T_c even at 5.5°K. The highest Si content on the 140° run with a measureable T_c onset above 5.5°K was at

20 [at.%] Si. Figure 12 shows the structure at this composition. It was the maximum disordering permissible in A15 to give a T_c above 5.5°K. The samples with various deposition temperatures and compositions were then annealed for 24 hrs. at 570°C. No change in structure was observed. A second anneal for 24 hrs. at 680°C however showed some important changes in structure. New lines of tetragonal Nb_3Si [6] were observed in all the samples. Samples with compositions less than 25 at.% Si showed additional lines of A2 (b.c.c.) phase and samples higher than 25 at.% Si showed the line systems of Nb_5Si_3 [19] phase. Samples with amorphous structure at 25 at.% Si had transformed into A15 + tetragonal after anneal. Whereas samples with A15 structure at the same composition had sharper A15 lines + tetragonal lines after annealing. It is proposed that the two reactions were as follows:

$$\text{i)}\quad \text{Amorphous} \xrightarrow[24\text{ hrs}]{680^\circ\text{C}} \text{A15 (disordered)} + \text{Tetragonal}$$

$$\text{ii)}\quad \text{A15 (disordered)} \xrightarrow[24\text{ hrs}]{680^\circ\text{C}} \text{A15 (partly ordered)} + \text{Tetragonal}$$

The tetragonal phase in the reaction (i) was more than in (ii). Samples deposited at 140°C which had the amorphous phase starting at a composition a little higher than 20 at.% Si, had shifted the amorphous growth to 30 at.% Si after the anneal and the T_c changed from unmeasurable (i.e. below 5.5°K) to 8.3°K at this composition. The T_c of samples with initial A15 did not show any improvement in T_c.

Samples deposited at different temperatures with 25 at.% Si were then annealed at 620°C for 24 hrs. Samples with deposition temperatures as low as 200°C, which were amorphous at this composition, showed A15 growth, whereas samples with higher deposition temperatures had slightly sharper A15 lines. This observation provided motivation for annealing for a longer period of time to grow more A15 from the amorphous phase. Three samples were taken at 25 at.% Si with deposition temperatures at 450°C, 200°C and 140°C, and annealed for 170 hrs at 640°C. Then the 450°C deposition temperature sample had well ordered A15 (compared to 24 hrs anneal at 620°C), but the other two samples had decomposed to A15 + Tetragonal. These data are compiled as follows:

Table VIII. Structures before and after anneal (640°C - 170 hrs) as a function of deposition temperature.

At.% Si	Deposition Temperature	Structure	
		Before Anneal	After Anneal
25	450	A15	A15 lines were narrower
25	220	Amorphous	A15 + Tetragonal + Amorphous
25	140	Amorphous	A15 + Tetragonal + Amorphous

The data indicated that this anneal resulted in the growth of the tetragonal phase from the amorphous phase, whereas the A15 to tetragonal transformation was slower. A 24 hrs anneal at 720°C showed growth of tetragonal from the A15 phase. The observations made in this anneal were as follows:

Annealed for 24 hrs. at 720°C

	At.% Si	Deposition Temperature	Structure	
			As Deposited	After Anneal
1)	25	220°C	Amorphous	A15 + Large amount of Tetragonal
2)	25	450°C	A15	Large amount of A15 + Tetragonal

Figures 13 and 14 show the samples 1 and 2 after the anneal. The amorphous phase had much more tetragonal than the A15 after the anneal. The T_c measured on these samples showed no T_c onset even at 5.5°K. The growth of tetragonal had deteriorated the T_c values. The decomposition of amorphous to A15 + Tetragonal after 170 hrs anneal at 640°C whereas the A15 remained A15, cannot be explained by free energy consideration. Kinetics play an important role in these reactions. Besides the rate of nucleation given by free energy considerations, growth rate, which is controlled by diffusion, has to be considered as well. Since the amorphous phase decomposed to A15 + Tetragonal, whereas the A15 remained A15 after 170 hrs anneal at 640°C, it was thought that the 2 phases would have two different Time-Temperature-Transformation curves.

So, based on our limited number of experiments, an effort was made to draw a tentative TTT diagram, Fig. 15, of the amorphous to A15 and further to tetragonal transformation. Compiling the annealing data, the transformations of the amorphous phase occur as follows:

$$\text{Amorphous} \xrightarrow[24\text{ hrs}]{570^\circ\text{C}} \text{Amorphous} \xrightarrow[24\text{ hrs}]{620^\circ\text{C}} \text{A15} + \text{Amorphous} \xrightarrow[170\text{ hrs}]{640^\circ\text{C}}$$

$$\text{A15} + \text{Tetragonal} + \text{Amorphous} \xrightarrow[24\text{ hrs}]{680^\circ\text{C}} \text{A15(poor ordering)} + \text{Tetragonal}$$

$$\xrightarrow[24\text{ hrs}]{720^\circ\text{C}} \text{A15 (improved ordering)} + \text{Tetragonal (more)}$$

Since more tetragonal formed at 680°C than at 640°C, the tetragonal curve was believed to lie far from the A15 curve at this temperature, whereas, the transformation from A15 to tetragonal started at 680°C, and the ordering of A15 started when annealed at 640°C for 170 hours. A longer period of anneal would have given a better ordering of the A15 (until the tetragonal start curve was reached for this temperature).

It is thought that a better ordering can be done on as-deposited films. This would not only save the long period of annealing, but also the problem of holding the temperature constant between a very short range i.e. 640°C and 680°C. The amorphous phase forms at higher Si at.% compositions with increasing deposition temperatures. With decreasing Si content the amorphous phase changes to disordered A15, and then to better ordered A15. Since the highest T_c so far obtained was at 21 [at.%] Si on the 530°C deposition run, a higher deposition temperature would depress the amorphous formation to higher Si content

resulting in better ordered A15 at the 25 at.% Si composition and thereby have a high T_c. So a search should be made for this optimum temperature, i.e. the highest temperature of deposition where the films still have the A15 structure. If even at this temperature the 25 at.% Si composition does not have good ordering, then the above mentioned annealing should be carried out.

III. GENERAL DISCUSSION

The discrepancies in lattice parameter measurements and the low T_c values will be discussed next. It can be clearly seen from the Fig. 2(e) that the higher the deposition temperature, the greater is the deviation from Müller's values of lattice parameter obtained on bulk samples. The fact that the present data points lie close to the parallel lines suggests that the relative change of lattice parameters with respect to Ge content for a particular run is the same as observed by Müller. The increasing deviations in the absolute values of the lattice parameters with increasing deposition temperatures can be explained by considering the difference in the coefficient of thermal expansion of the substrate and the film deposit. If the substrate has a smaller coefficient of expansion than the deposited film, then the contraction of the film deposits on cooling would be prevented by the substrate. This would leave the films in a state of tension which would lead to high lattice parameter measurements for some planes. The lower the deposit temperature, the smaller the difference in contraction which leads to a lower tension and thus lower lattice parameter deviations from actual values. From these arguments it seems that lattice parameters comparable to those in bulk samples could be attained for low substrate temperature runs.

In Fig. 2(e) at the 16 at.% Ge composition the difference in lattice parameters between Muller's and our measurements at 600°C is $5.205\text{Å} - 5.170\text{Å} = 0.035\text{Å}$. The coefficient of linear expansion of the

superstrate is 10×10^{-6} per °C. The coefficients of linear expansion of our films are not known, but they lie between 5×10^{-6} per °C and 15×10^{-6} per°C for some known superconductors. Assuming ours is the highest value, we set up the equation

$$\frac{\Delta a_o}{a_o} = (15 - 10) \times 10^{-6} \times \Delta T$$

Since our film was deposited at 600°C we can approximately say

$$\frac{\Delta a_o}{a_o} = 5 \times 10^{-6} \times 600 = 30 \times 10^{-4}$$

$$\Delta a_o = 150 \times 10^{-4}\text{Å} = 0.015\text{Å}$$

Comparing this with the deviation of 0.035Å, we could justify only half the amount of deviation, even if all our assumptions were correct. But K. L. Chopra[20] has discussed the possibilities of such discrepancies in lattice parameter measurements made on thin films. Film thickness and the crystallite size seem to influence the lattice parameter to a great extent. A negative or positive deviation from the bulk measurements depend upon the surface energy. Boswell[21] has observed a 1% increase in the lattice constant for crystallites ranging from 30 to 100Å in size in LiF films. On the other hand a decrease in the lattice constants of evaporated alkali halide films with decreasing crystallite size was observed by Finch.[22] Furthermore K. L. Chopra suggests special techniques such as that of Moiré fringes should be

applied to measure the lattice constant accurately. Our crystallites were approximately 300Å, as measured from x-ray diffraction half peak widths.

Since the crystallite sizes are very much dependent on substrate temperatures, therefore from K. L. Chopra's view point our results are comprehensible. The relative change of lattice parameter with respect to the composition was the same for both the runs 600 and 420°C. This proves that the error is a systematic deviation and not random. These reasonings are also valid for Nb_3Ga lattice parameters.

The high lattice parameter measured in β-W Nb_3Si phase, as contrasted by what is expected by Geller's[23,24] calculation, can be attributed to the fact that the lattice parameter was measured on the 21 at.% Si composition, in a β-W Nb_3Si and Nb (b.c.c.) mixed phases. So it is a measure of the lattice parameter of the β-W Nb_3Si phase with the lowest Si solubility. It is quite possible that the errors due to film thickness and crystallite size, as discussed above are also included in this system.

Although success was achieved in extending the A15 phases in the NbGe and NbGa towards a 3:1 stoichiometric composition, the fact that superconducting values as high as those obtained by previous investigators were not attained can be attributed to the "noise" that was involved in the Nb evaporation. The fluctuations of the Nb rate was beyond the range of modulation of the feed back loop. This fluctuating rate of evaporation of the Nb resulted in an inhomogenity in composition through the thickness of the films. The annealing temperatures were not high enough to cause bulk diffusion, which could have homogenized

the films. The broad transitions, which were sometimes more than 3°K, are also due to the inhomogenous films. Better control of the niobium flux at high rates of deposition is very important for the making of homogeneous films. It is expected that better control would lead to better ordered A15 compounds, and thus to a true value of their critical temperatures.

ACKNOWLEDGEMENTS

The work was made possible through the support of Professors Leo Brewer, Earl R. Parker and Victor F. Zackay. Professors Earl Parker and Victor Zackay offered many helpful suggestions and encouragement during the progress of this work. Thanks are due to Larry Hartsough and Mike Collver who contributed their experience in electron beam evaporation and many helpful discussions.

I feel indebted to Dr. Robert H. Hammond for his scientific advice, friendliness and encouragement which he extended through our day-to-day work together.

I express my gratitude to Mr. Hermann C. Starck and Mr. Fred Lenway for their support during part of the study.

This work was done under the auspices of the United States Atomic Energy Commission.

REFERENCES

1. A. Muller, Z. Naturforscer 25A, 1659-69 (1970).

2. B. T. Matthias, T. H. Geballe, R. H. Williams, E. Corenzwit and G. W. Hull, Jr., Phys. Rev. 139A, 1501 (1965).

3. G. W. Webb, L. J. Vieland, R. E. Miller and A. Wicklund, David Sarnoff Research Center RCA Laboratories, Princeton, New Jersey (to be published.)

4. J. J. Hopfield, (to be published).

5. M. V. Nevitt, in Paul A. Beck, ed., Electronic Structure and Alloy Chemistry of the Transition Elements, (Interscience, 1962), p. 101.

6. D. K. Deardorff, R. E. Siemens, P. A. Romans and R. A. McCune, Journal of Less Common Metals, Vol. 18 (1969).

7. F. Galasso and J. Pyle, Acta Cryst. 16 (1963), 228.

8. L. D. Hartsough and R. H. Hammond, Solid State Communications, Vol. 9, (1971), pp. 885-889.

9. J. Philbert, L. Analyse Quantitative en Microanalyse par Sonde Electronique, (IRSID Publ., Series B, No. 51, 1965).

10. P. Duncumb and P. K. Shields, Effect of Critical Excitation Potential on the Absorption Correction in X-Ray Microanalysis, (Tube Investments Research Laboratories, Technical Report No. 181).

11. H. Bishop, Brit. J. Appl. Phys (J. Phys. D.) I (1968), 673.

12. K. F. J. Heinrich in The Electron Microprobe, T. McKinley, K. Heinrich and D. Whittey, eds., (Wiley, New York, 1966), p. 284.

13. M. V. Nevitt, Trans. AIME 212, 350 (1958).

14. P. Duwez and R. H. Willus, Trans. Met. Soc. AIME 227, 362 (1963).

15. W. Buckel and R. Hilsch, Z. Physik 138, 109 (1954).
W. Buckel, Z. Physik 138, 136 (1954).

16. R. Hilsch, in Noncrystalline Solids, V. D. Frechette, ed., (Wiley, New York, 1960), Ch. 15.

17. S. Mader, A. S. Nowick and H. Widmer, Acta Met. 15, 203 (1967).

18. V. V. Baron, L. F. Myzenkova, E. M. Sairtsky and E. I. Gladyshevskiy, J. Inorg. Chem. 9 (1962), 1172.

19. Parthe, et al., Monatsh. Chem. 86, 859 (1955).

20. K. L. Chopra, Thin Film Phenomena, (McGraw-Hill Book Co., 1969).

21. F. W. C. Boswell, Proc. Phys. Soc. London A64, 465 (1951).

22. G. I. Finch and S. Fordham, Proc. Phys. Soc. London 48, 85 (1936).

23. S. Geller, Acta Cryst. 9, 885 (1956).

24. S. Geller, Acta Cryst. 10, 380 (1957).

FIGURE CAPTIONS

Fig. 1 (a) Schematic of the circuit used to measure the resistance of the samples. (b) Schematic of the circuit used to measure the resistance of the germanium thermometers.

Fig. 2 (a) Ge at. % of the Ge rich side A15 phase boundary vs. deposition temperatures. (b) Lattice parameters on the A15 phase boundary vs. Ge at. %. (c) T_c peaks at the phase boundary vs. Ge at. % as deposited. (d) T_c peaks at the phase boundary vs. Ge at. % after 24 hrs anneal at 700°C. (e) Lattice parameter vs. at.% Ge, measured on samples with 600°C (A' B') and 420°C (C' D') deposition temperatures. AB corresponds to Müller's observations.

Fig. 3 X-ray diffraction pattern of the A15 Nb_3Ge phase at the phase boundary on the sample deposited at 300°C.

Fig. 4 X-ray diffraction pattern of the A15 Nb_3Ge phase at the phase boundary on the sample deposited at 420°C.

Fig. 5 X-ray diffraction pattern taken on 300°C run after 700°C anneal for 24 hrs at the A15 Nb_3Ge phase boundary.

Fig. 6 (a) Deposition temperature vs. at. % Ga and lattice parameter measured at the A15 phase boundary (Ga rich side). (b) T_c peaks at the phase boundary vs. at. % Ga and lattice parameter on as deposited films. (c) T_c peaks at the phase boundary (Ga rich side) vs. at. % Ga after 24 hrs anneal at 700°C.

Fig. 7 X-ray diffraction pattern taken at 30 at. % Ga composition on 'as deposited' film.

Fig. 8 X-ray diffraction pattern taken at 30 at. % Ga composition after 24 hrs anneal at 700°C.

Fig. 9 A Laue Transmission pattern taken on the β-W Nb_3Si phase at 21 at. % Si composition.

Fig. 10 (a-e) X-ray diffraction pattern of the 100°C run, on as deposited film, at 11, 15, 17, 25 and 36 at. % Si respectively.

Fig. 11 X-ray diffraction pattern of the 530°C run at 25 at. % Si, as deposited.

Fig. 12 X-ray diffraction pattern of the 140°C run at 20 at. % Si, as deposited.

Fig. 13 X-ray diffraction pattern of the 220°C run at 25 at. % Si after an anneal for 24 hrs at 720°C.

Fig. 14 X-ray diffraction pattern of the 450°C run at 25 at. % Si after an anneal for 24 hrs at 720°C.

Fig. 15 Schematic TTT diagram of the amorphous ⟶ A15 + tetragonal transformation.

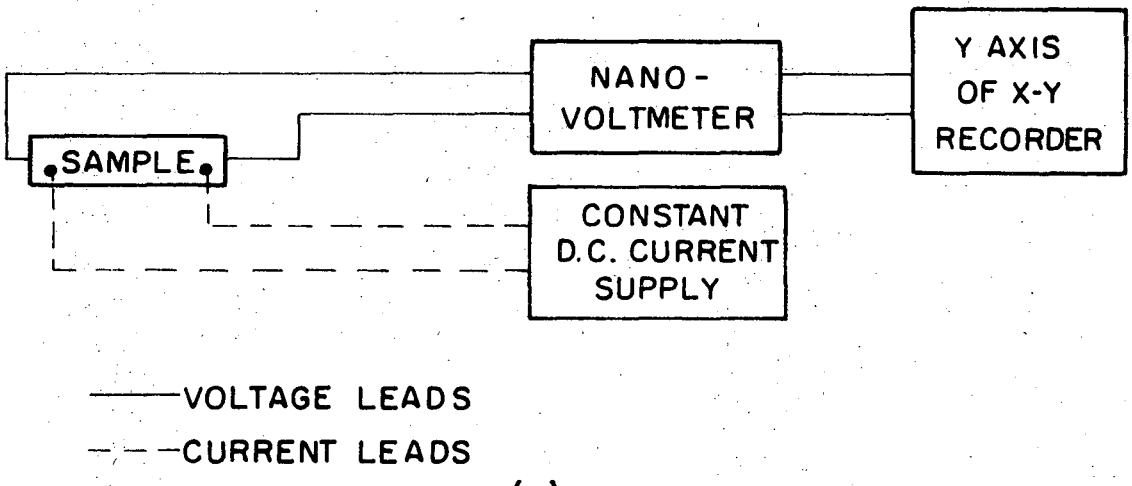

(a)

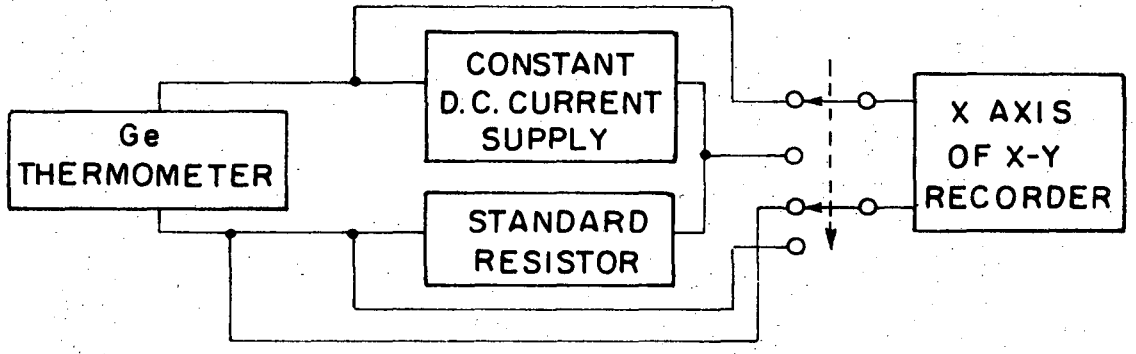

(b)

XBL7110-7428

Fig. 1.

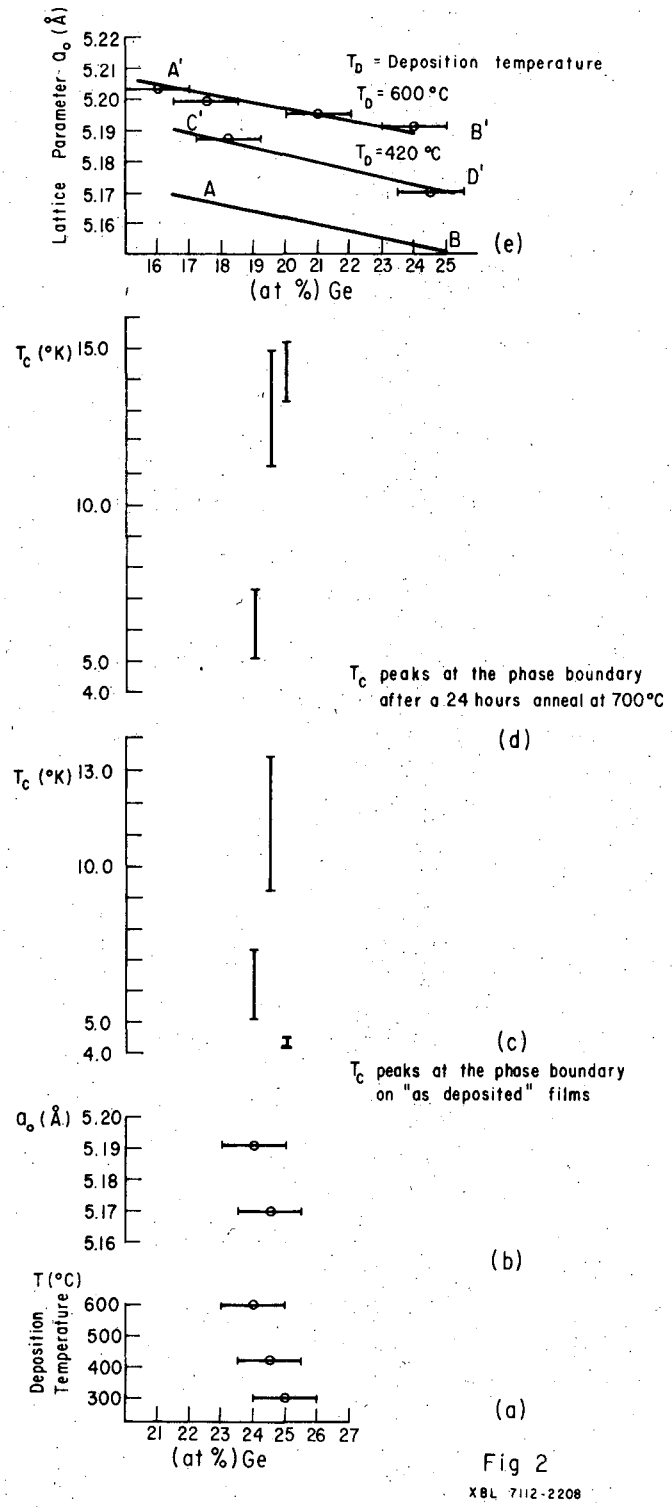

Fig 2

XBL 7112-2208

Fig. 2

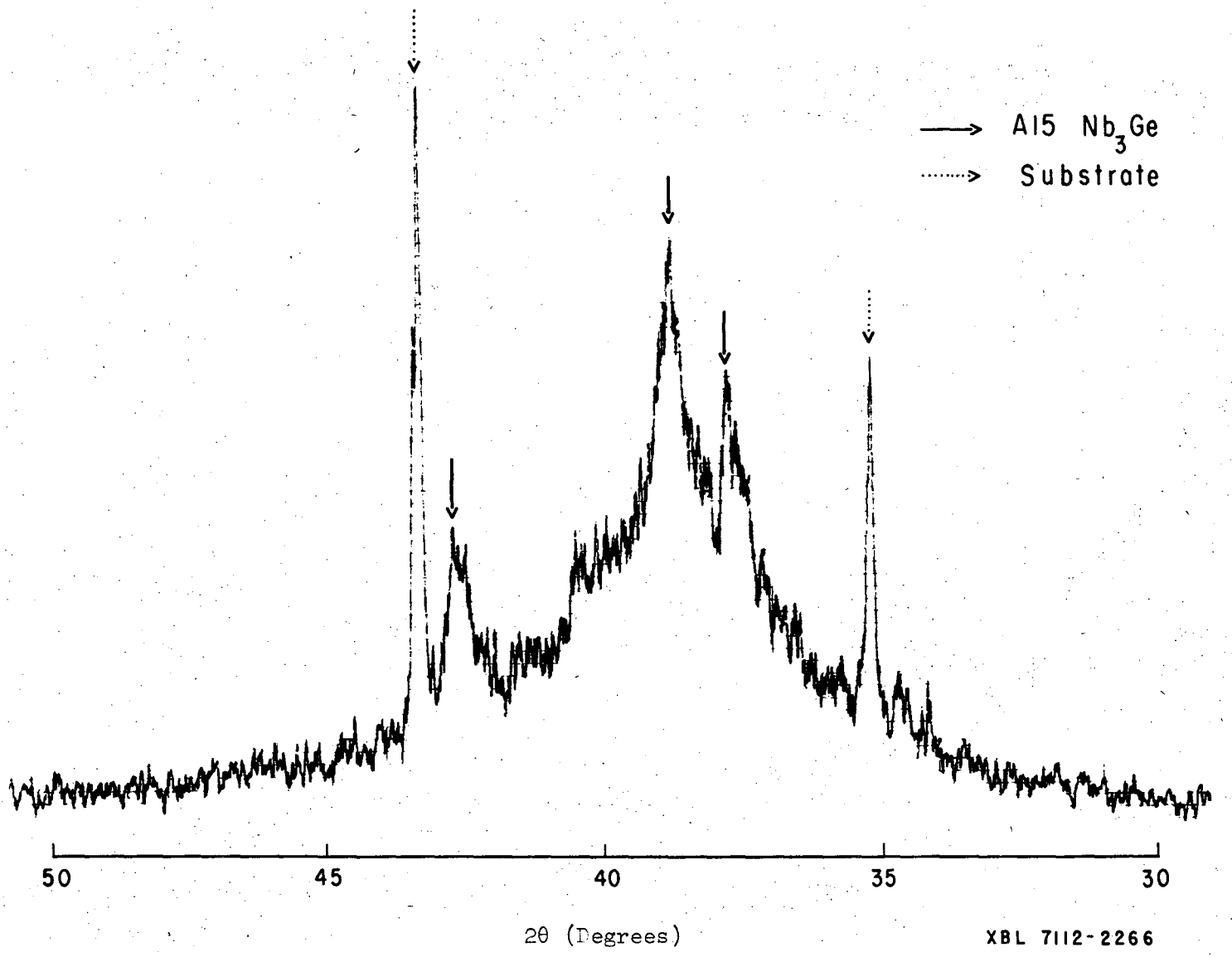

Fig. 3.

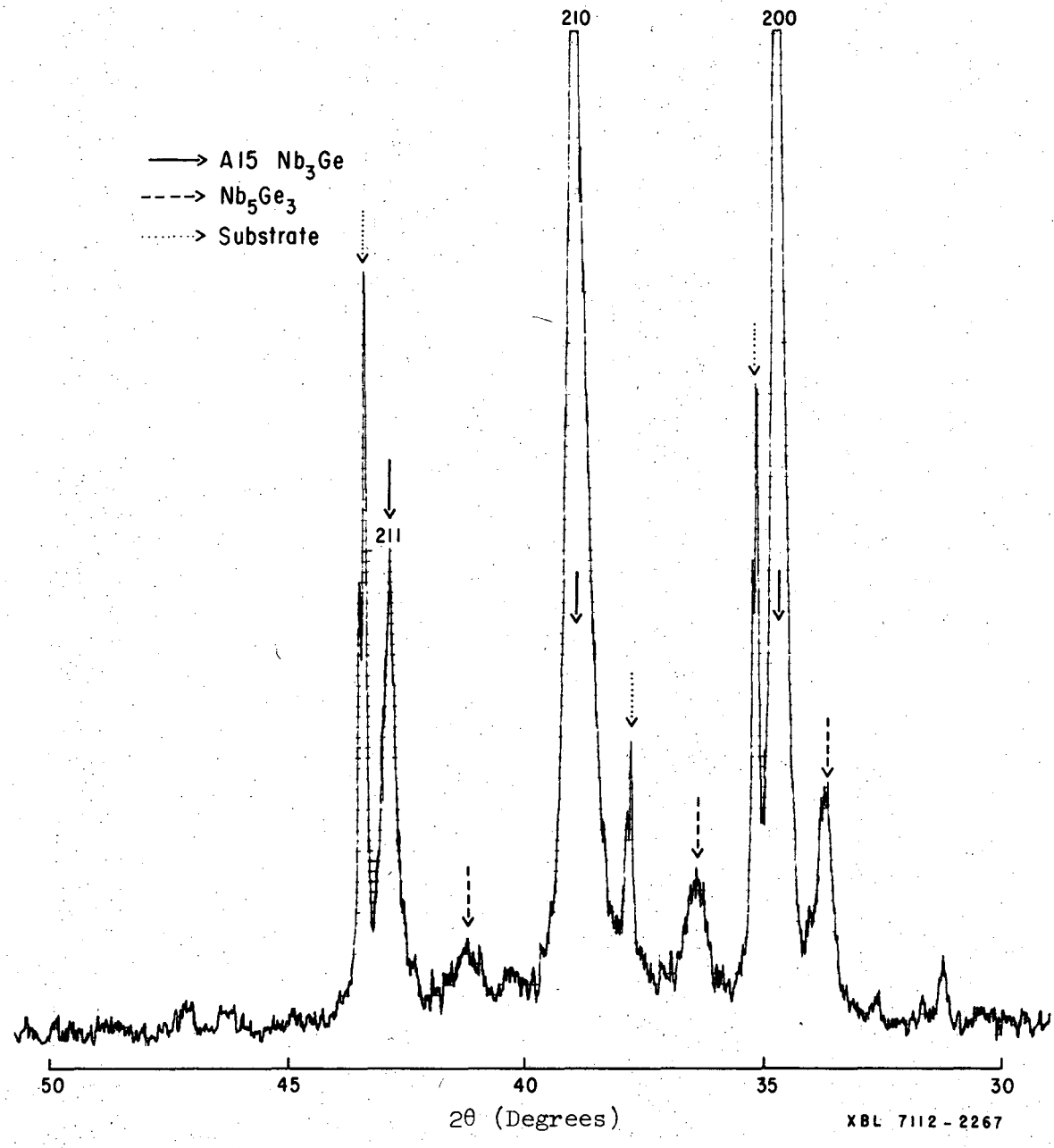

Fig. 4.

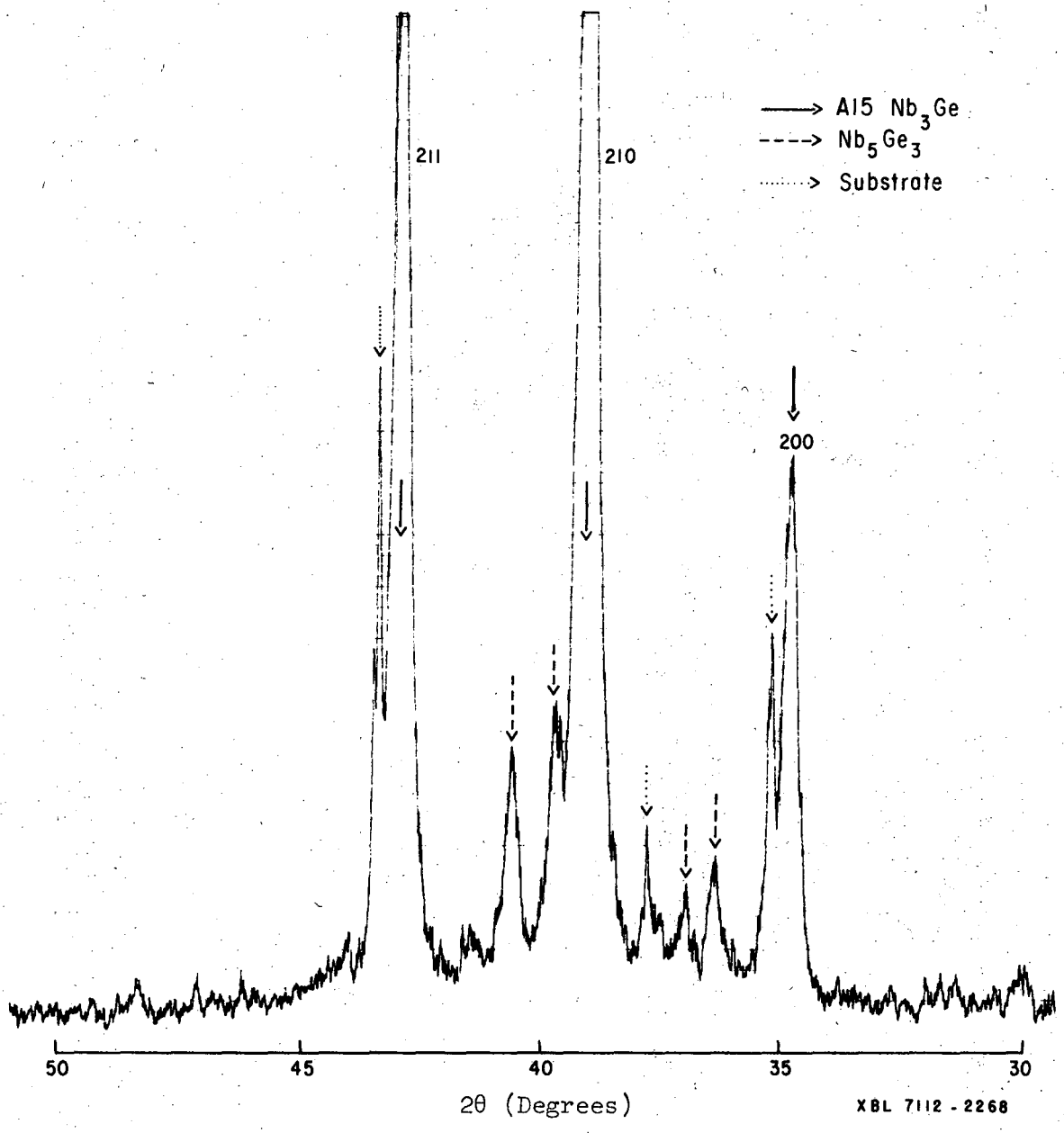
A15 Nb3Ge
Nb5Ge3
Substrate
211
210
200
50
45
40
35
30
2θ (Degrees)
XBL 7112 - 2268

Fig. 5.

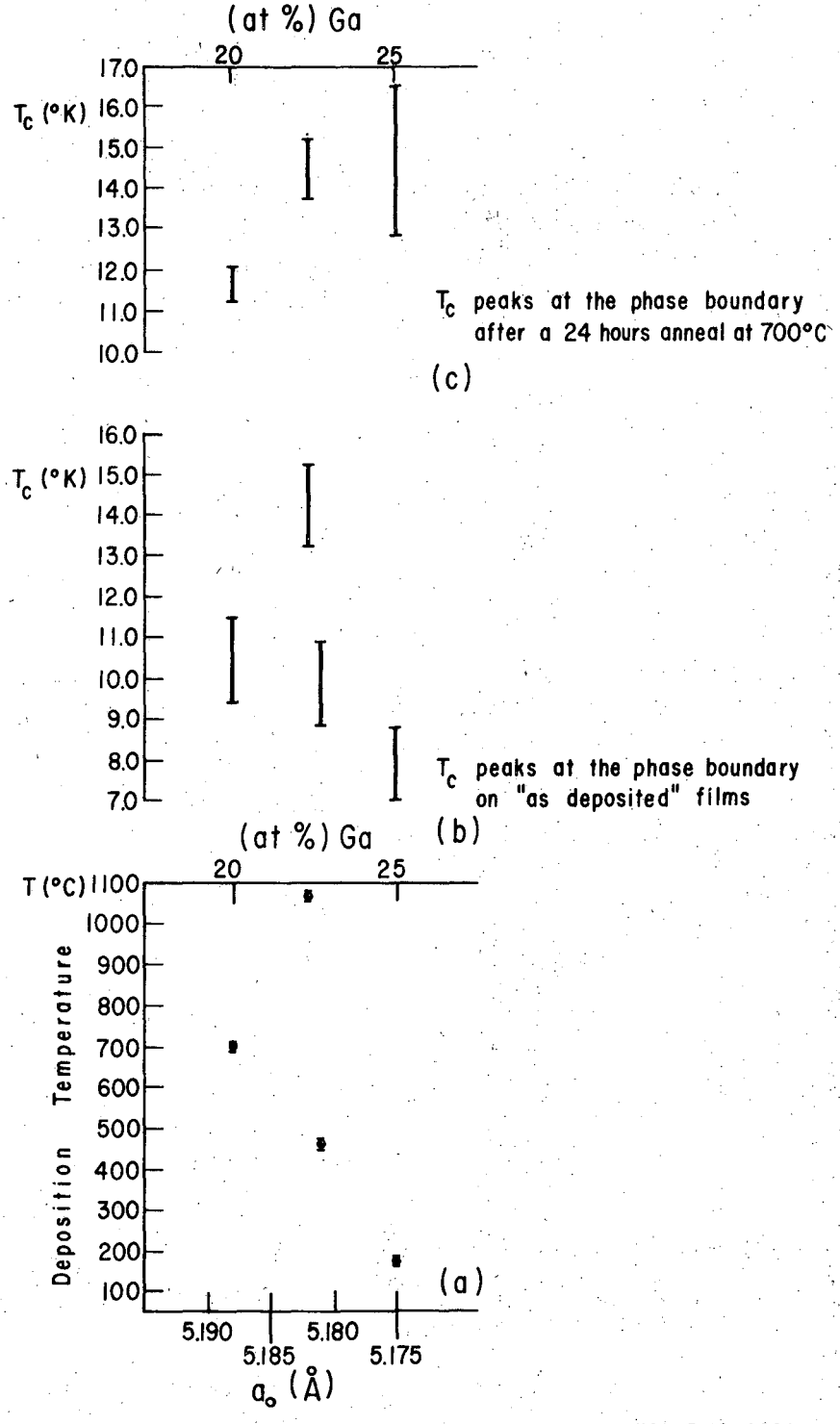
(at %) Ga
20
25
17.0
16.0
15.0
14.0
13.0
12.0
11.0
10.0
T_c (°K)
T_c peaks at the phase boundary after a 24 hours anneal at 700°C
(c)
16.0
15.0
14.0
13.0
12.0
11.0
10.0
9.0
8.0
7.0
T_c (°K)
T_c peaks at the phase boundary on "as deposited" films
(b)
(at %) Ga
20
25
T (°C) 1100
1000
900
800
700
600
500
400
300
200
100
Deposition Temperature
(a)
5.190
5.185
5.180
5.175
a_o (Å)
XBL 7112-2209

Fig. 6.

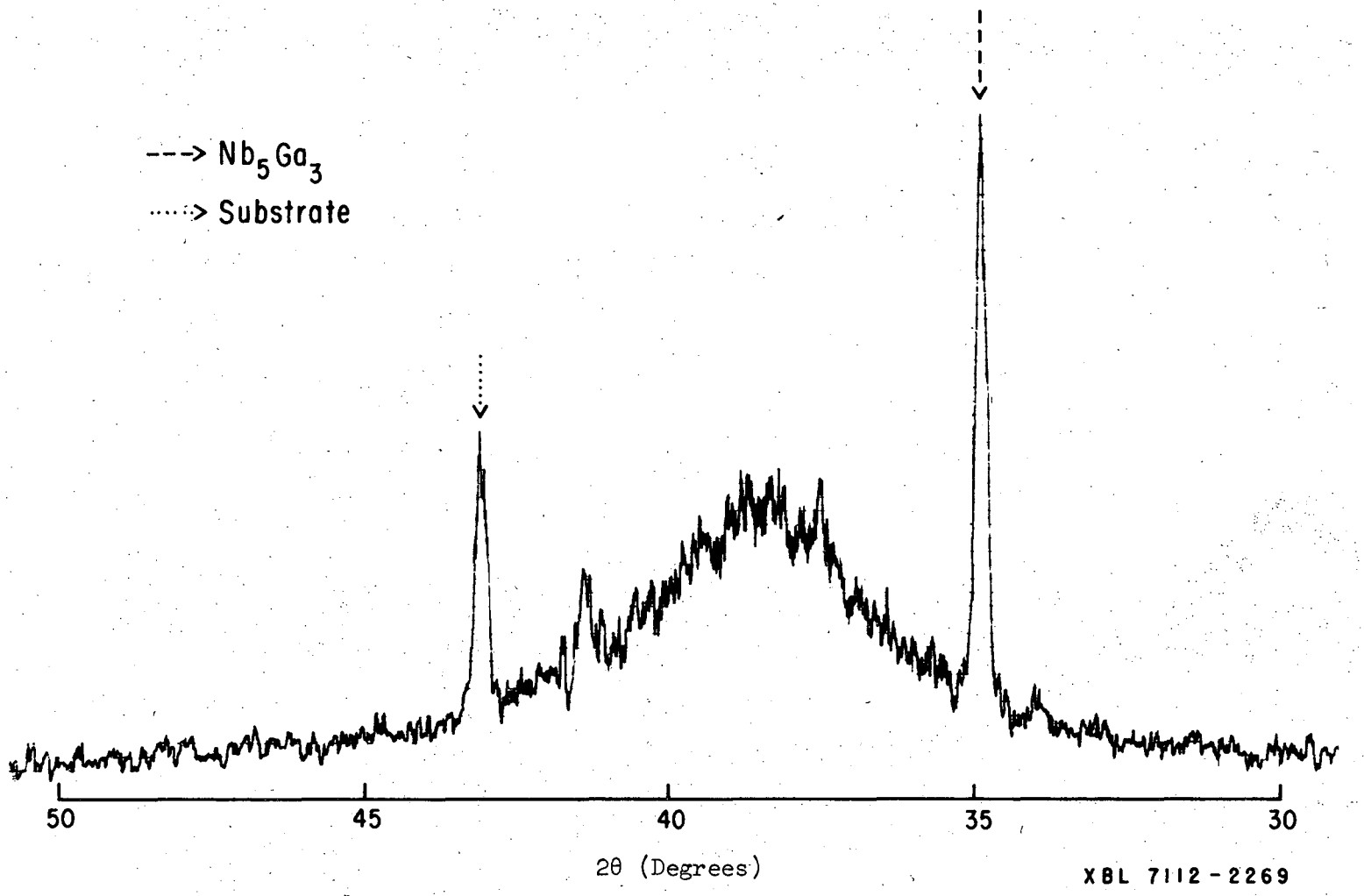

Fig. 7.

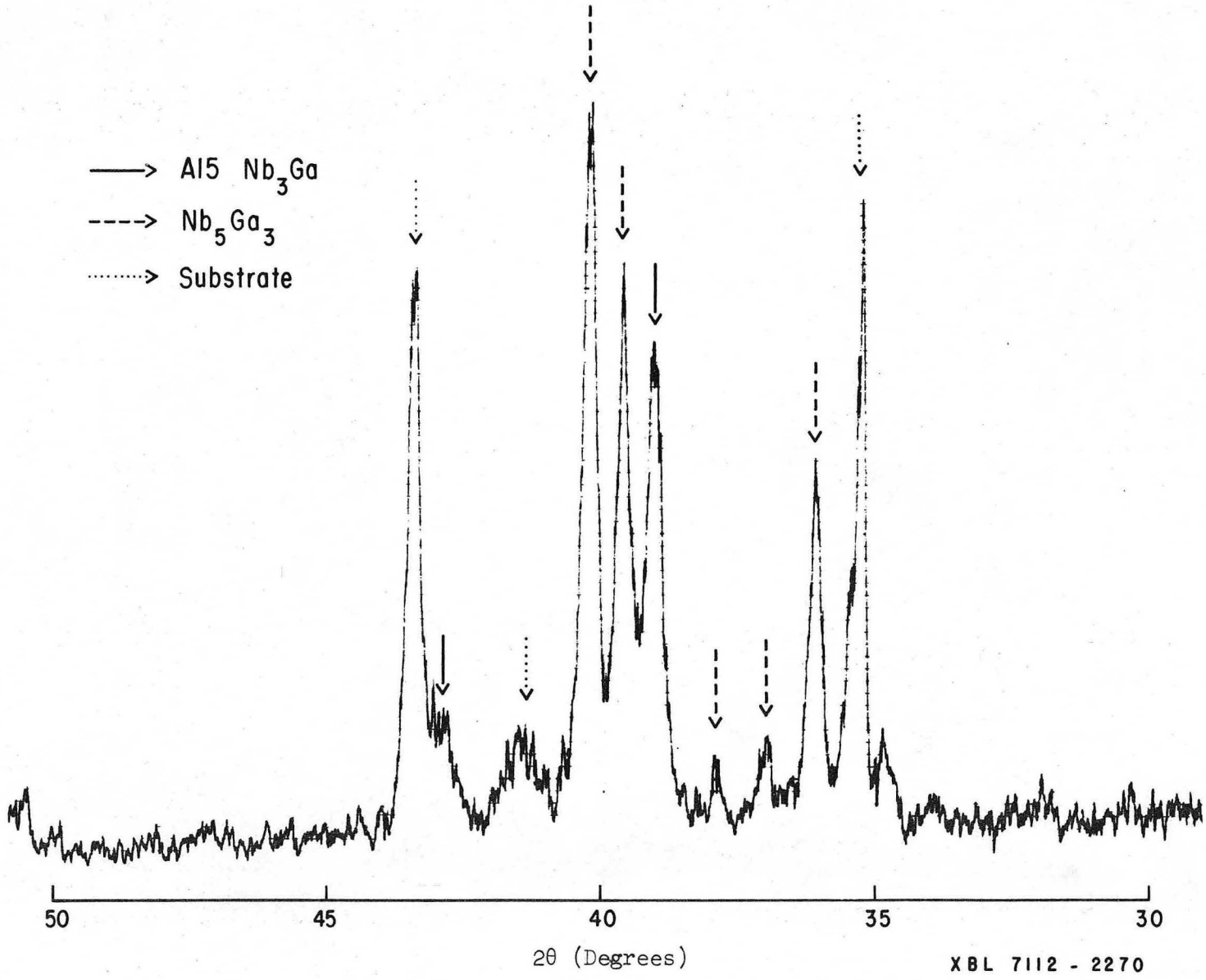
A15 Nb_3Ga
Nb_5Ga_3
Substrate
50
45
40
35
30
2θ (Degrees)
XBL 7112 - 2270

Fig. 8.

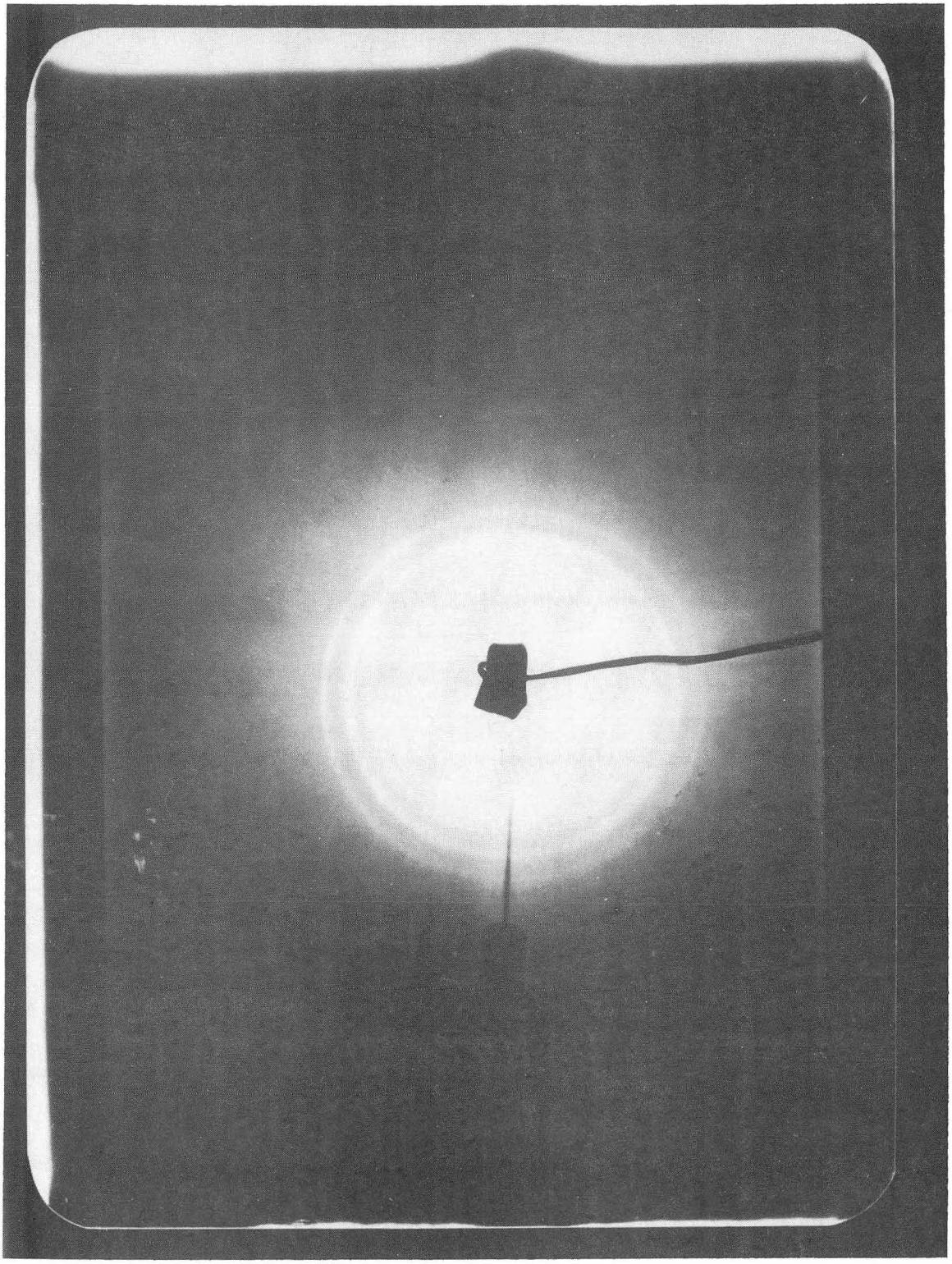

XBB 7112-6022

Fig. 9.

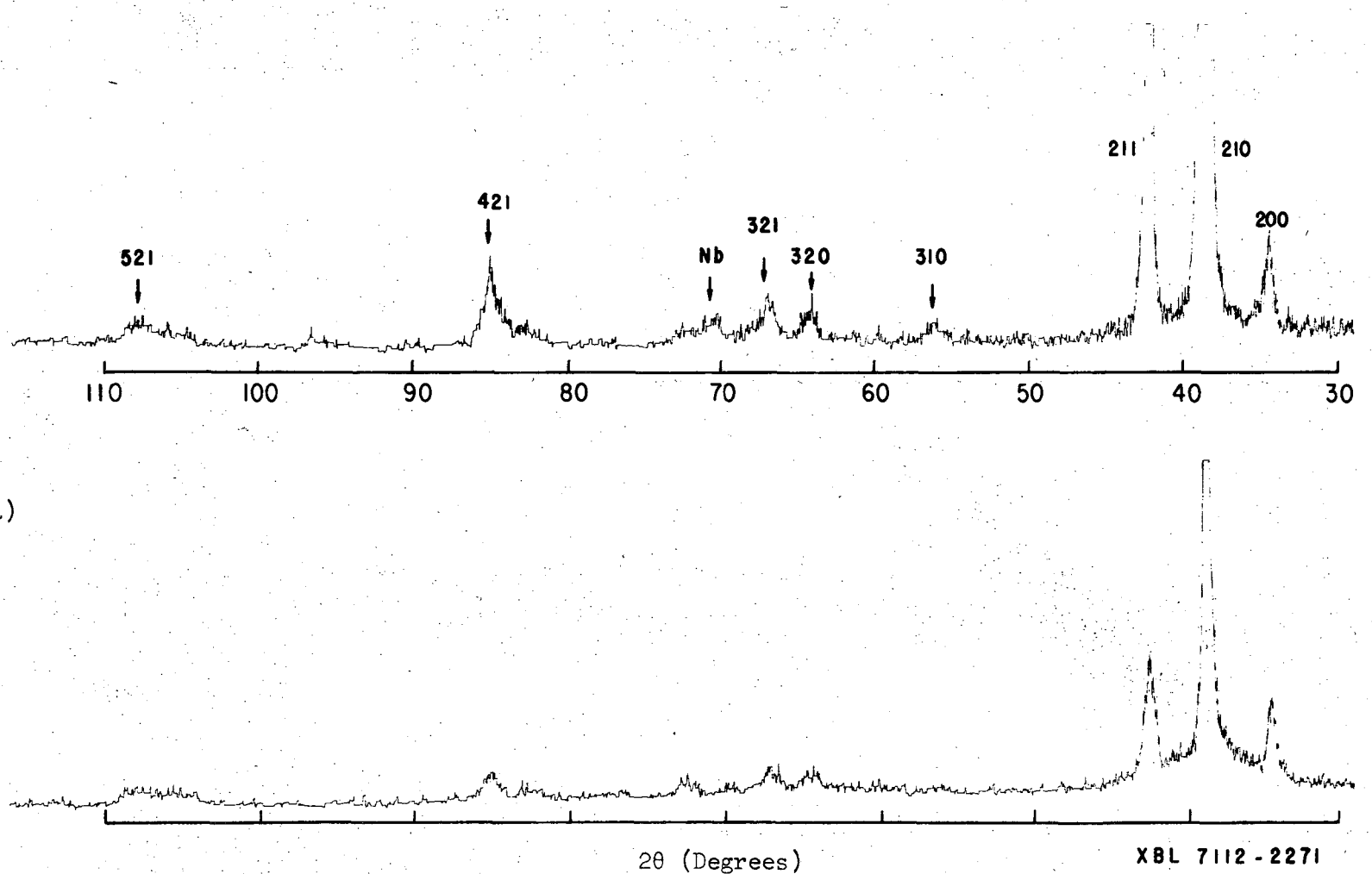
521
421
Nb
321
320
310
211
210
200
110
100
90
80
70
60
50
40
30
(a)
2θ (Degrees)
XBL 7112-2271
(b)

Fig. 10.

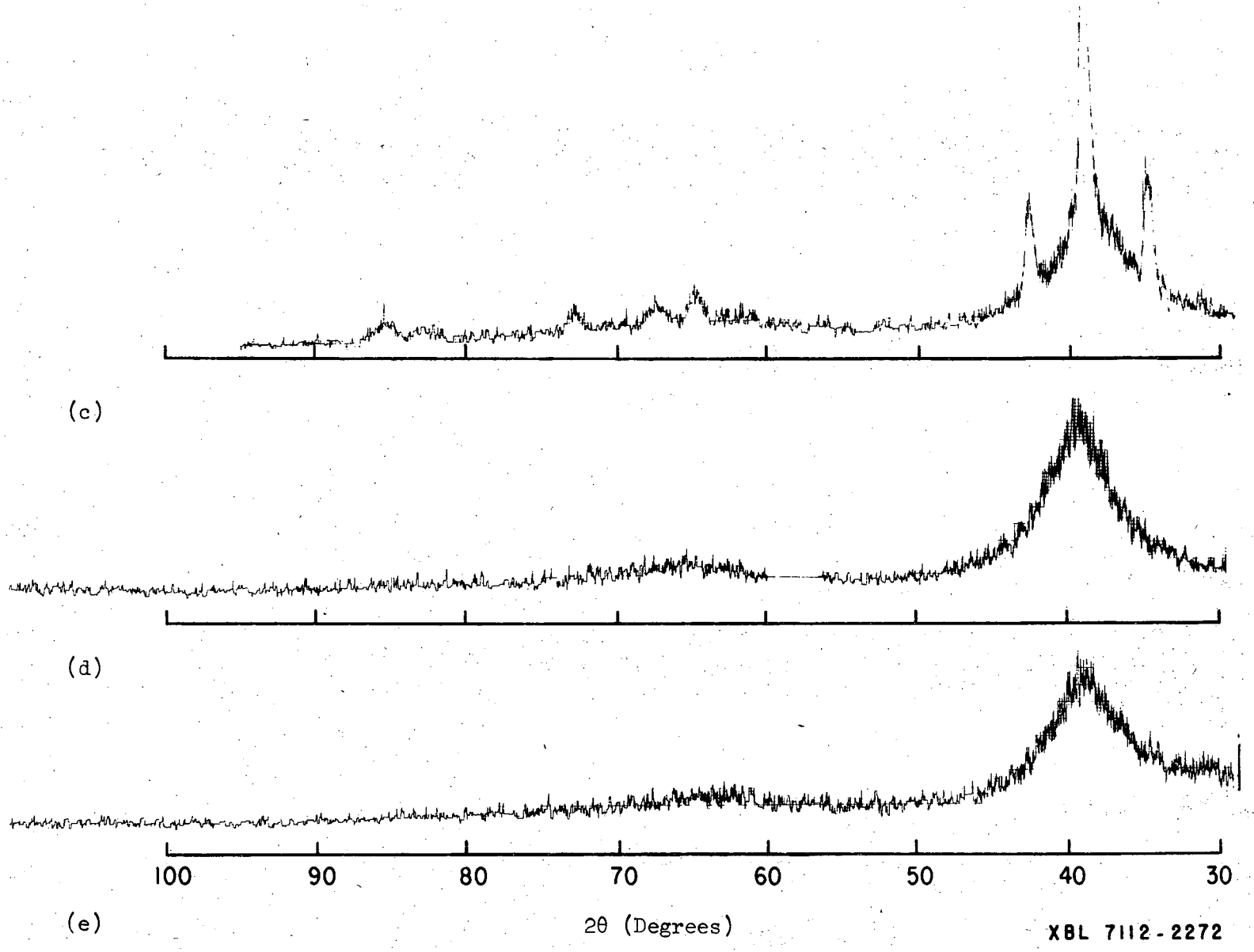

Fig. 10 (continued)

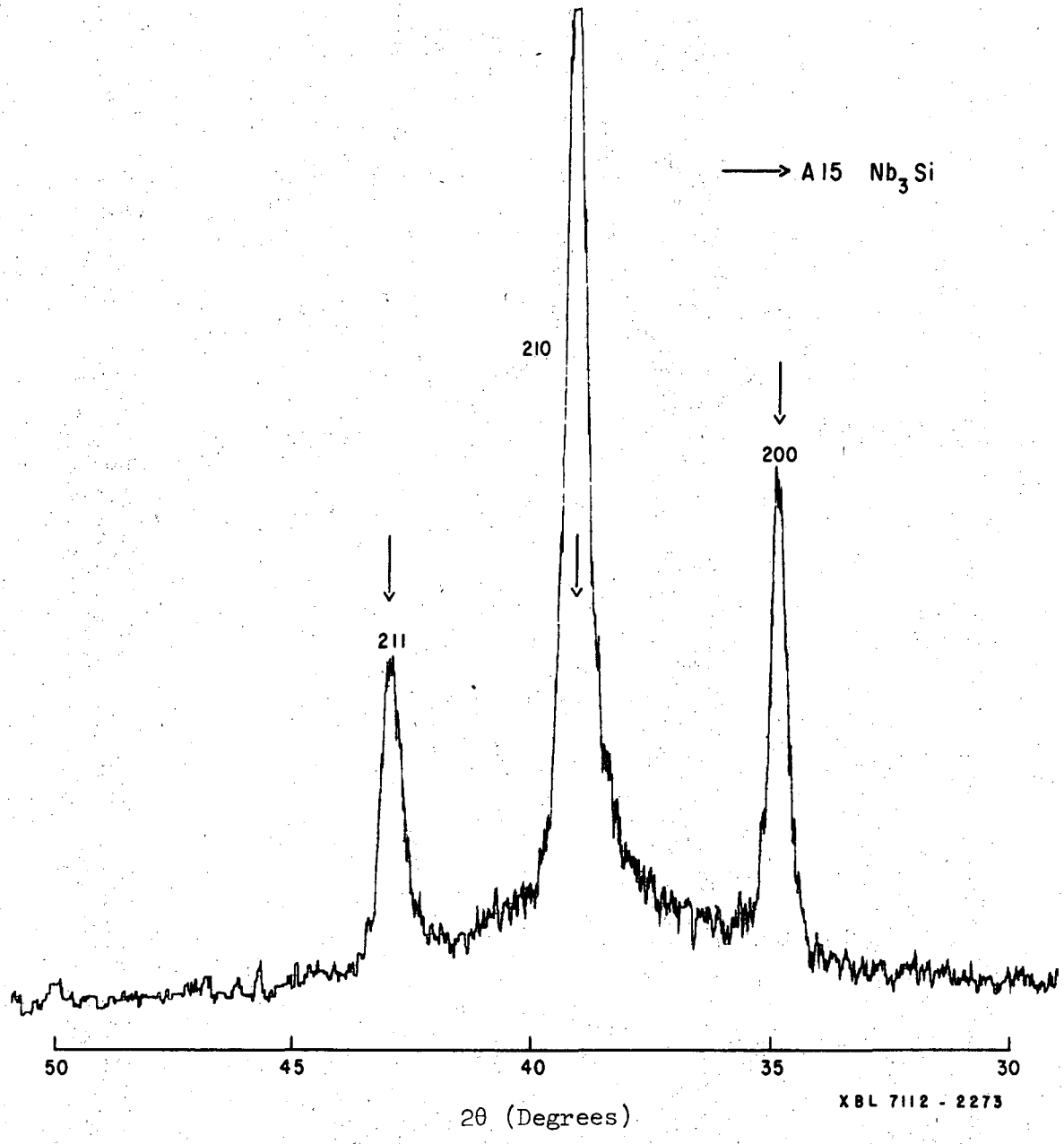

Fig. 11.

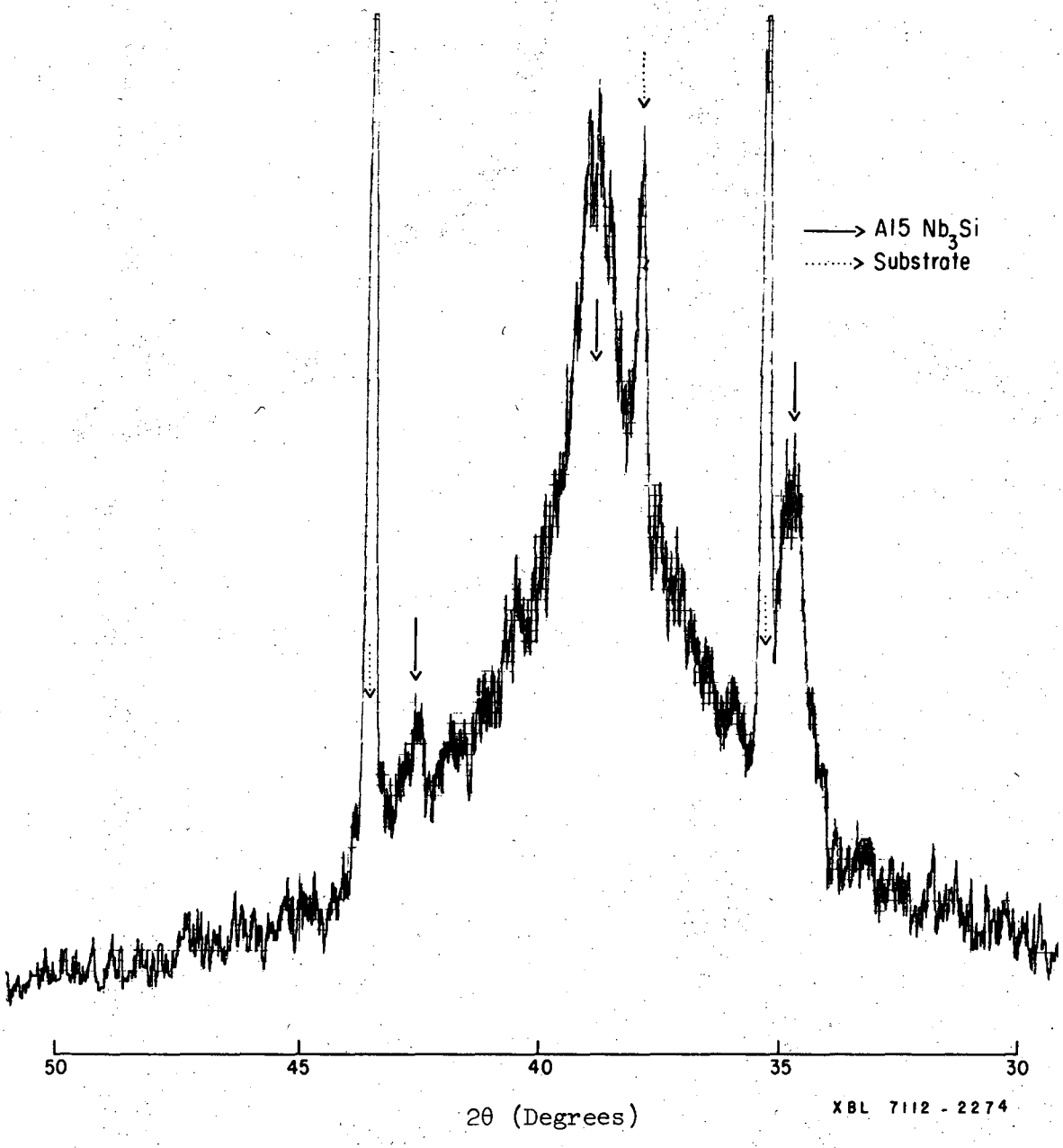

Fig. 12.

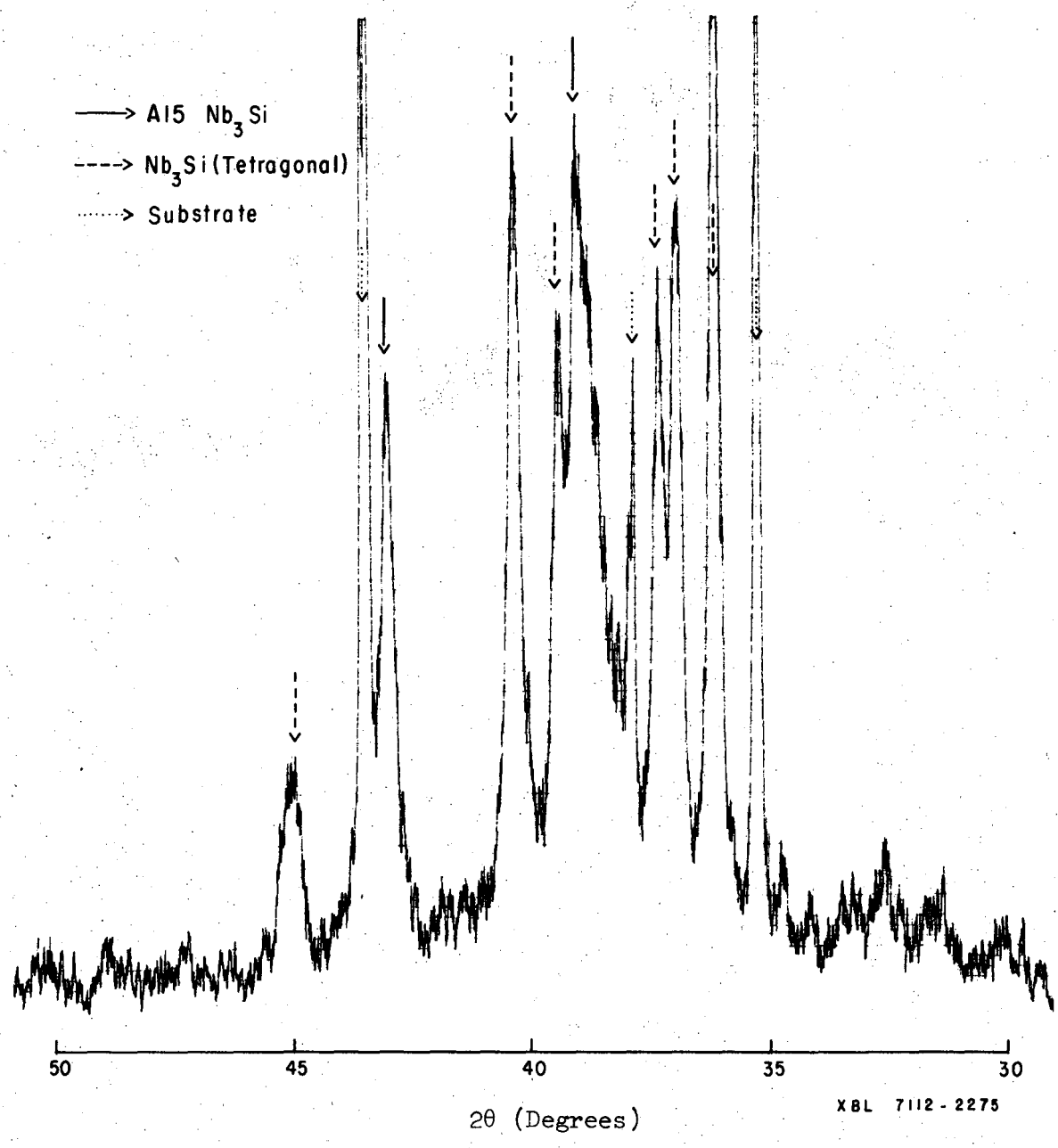
A15 Nb_3Si
Nb_3Si (Tetragonal)
Substrate
50
45
40
35
30
2θ (Degrees)
XBL 7112-2275

Fig. 13.

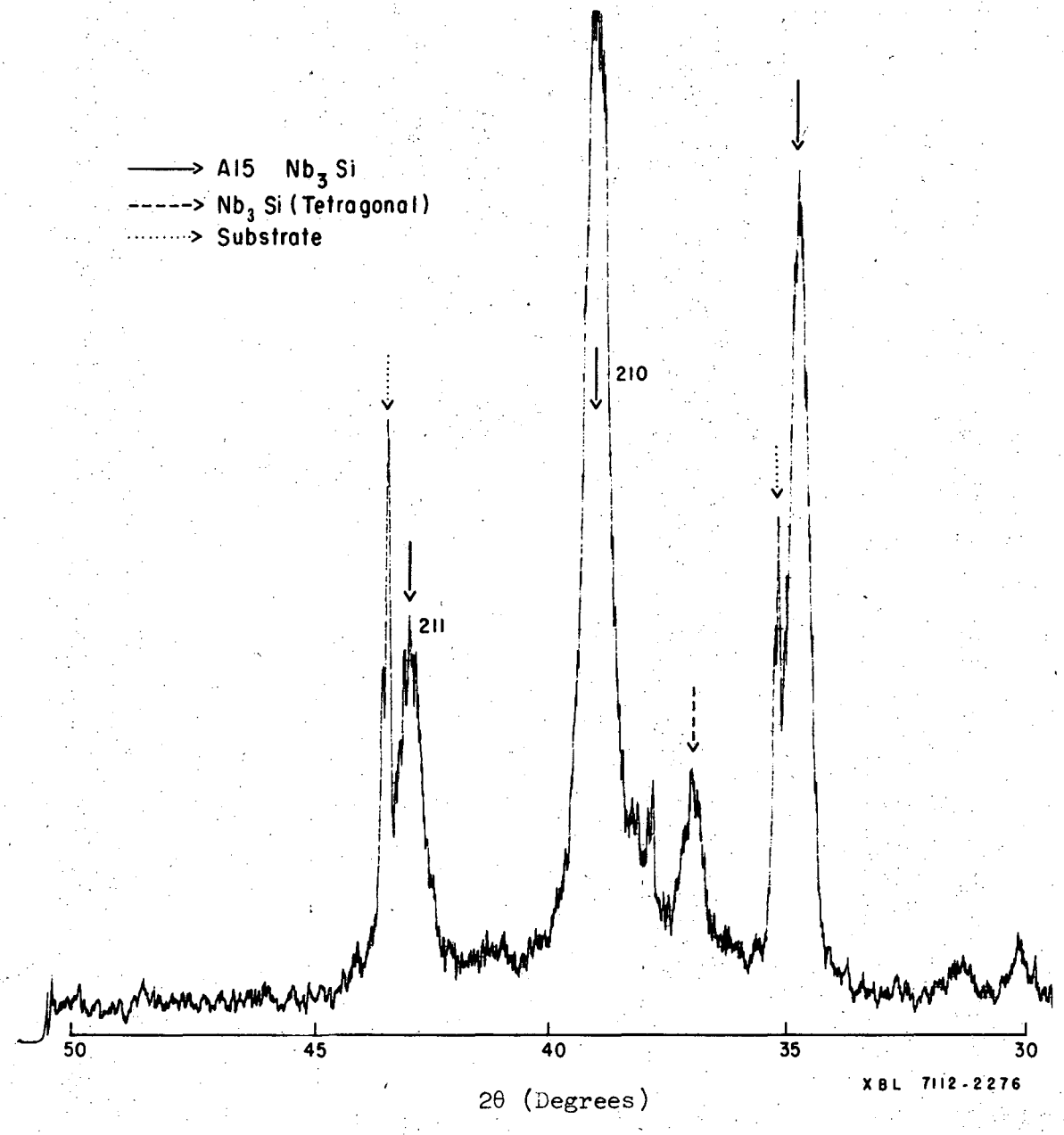
A15 Nb_3Si
Nb_3Si (Tetragonal)
Substrate
210
211
50
45
40
35
30
2θ (Degrees)
XBL 7112-2276

Fig. 14

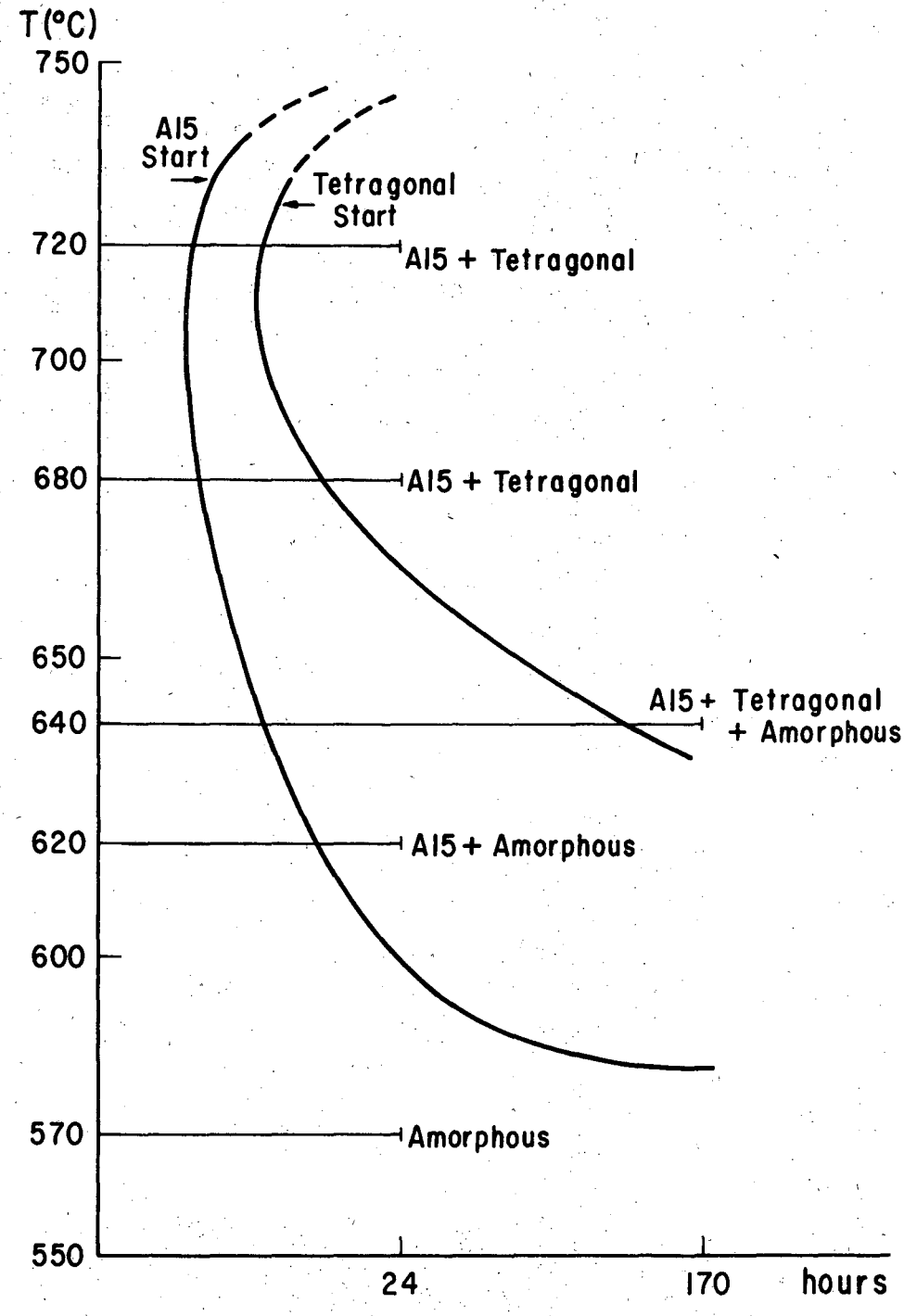

Fig. 15

XBL 7112-2228

TECHNICAL INFORMATION DIVISION
LAWRENCE BERKELEY LABORATORY
UNIVERSITY OF CALIFORNIA
BERKELEY, CALIFORNIA 94720